



# Multi-element contamination in soils from major mining areas in Northeastern of Brazil

D. M. Montalván-Olivares · C. S. Santana · F. G. Velasco · F. H. M. Luzardo · S. F. R. Andrade · R. B. Ticianelli · M. J. A. Armelin · F. A. Genezini

Received: 13 November 2020 / Accepted: 10 April 2021 / Published online: 26 April 2021  
© The Author(s), under exclusive licence to Springer Nature B.V. 2021

**Abstract** Mining has become one of the main factors in the global biogeochemical cycle of potentially toxic elements. Therefore, it is considered one of the anthropogenic activities with the greatest negative impact on the environment. These impacts are maximized in semiarid regions, where mining activities can lead to soil degradation and decrease in land productivity. This study aimed to assess the level of contamination in natural, urban, and agricultural soils of three important mining areas, where approximately 80,000 people live, and pollution levels have never been determined before. For this purpose, soil samples were collected around iron, uranium, and vanadium mines, as well as in the main human settlements of the region. The concentrations of 34 elements were

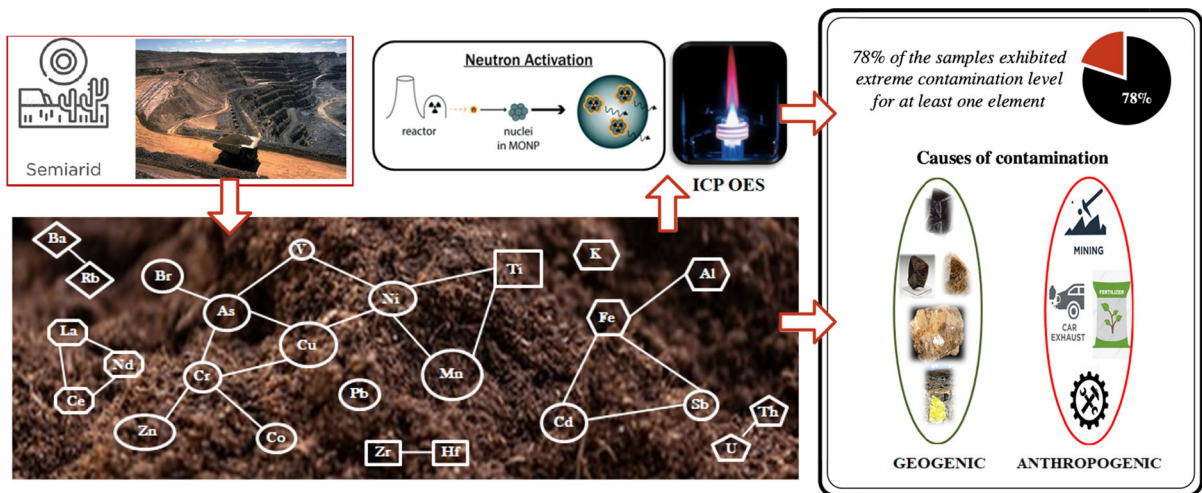
determined by instrumental neutron analysis activation (INAA) and inductively coupled plasma optical emission spectrometry (ICP OES) techniques. Pollution indices (CF, EF,  $mC_d$ , PLI, and REEP) revealed that there is a moderate to heavy level of pollution for 89% of the analyzed elements. Additionally, an extreme contamination level was observed in 78% of the samples, for at least one element. Statistical analyses were performed to identify patterns in the distribution and common sources of pollution. The results suggest that the concentrations for Al, Ba, Hf, Na, Pb, Rb, REE, Ta, Th, U, Zn, and Zr are associated with geogenic causes. However, the influence of anthropogenic sources such as agriculture and mining on the accumulation of these elements in soils should not be disregarded. In contrast, the contents of As, Br, Cd, Co, Cr, Cs, Cu, Fe, K, Mn, Ni, Sc, Ti, and V reflect the direct impact of anthropogenic sources.

**Supplementary information** The online version contains supplementary material available at <https://doi.org/10.1007/s10653-021-00934-x>.

D. M. Montalván-Olivares (✉) · C. S. Santana · F. G. Velasco · F. H. M. Luzardo · S. F. R. Andrade  
Center for Research in Radiation Sciences and Technologies (CPqCTR), State University of Santa Cruz (UESC), Highway Jorge Amado km 16, Ilhéus, Bahia 45662-900, Brazil  
e-mail: diango.mo87@gmail.com

R. B. Ticianelli · M. J. A. Armelin · F. A. Genezini  
Instituto de Pesquisas Energéticas e Nucleares, IPEN, CNEN/SP, Av. Prof. Lineu Prestes 2242, São Paulo 05508-000, Brazil

## Graphic abstract



**Keywords** Soil analysis · Trace elements · Neutron activation analysis · ICP OES · Anthropogenic impacts

## Introduction

The current growth of human society is strongly related to a process of progressive industrialization and greater exploitation of natural resources. Anthropogenic activities are contributing to an accelerated process of environmental pollution since they are responsible for the introduction and redistribution of potentially toxic elements (PTE) and naturally occurring radioactive materials (NORM) into ecosystems (Doležalová et al., 2019). There are a significant number of research works dedicated to the assessment of pollution by these inorganic pollutants, which reveals the great importance given by the scientific community to this topic (Fordyce et al., 2019; Kumar et al., 2017; Li et al., 2014; Wang et al., 2019). In general, these works show that the sources of contamination for these pollutants are diverse and that in the last ten years there has been a drastic increase in their concentrations in different environmental matrices (soil, sediments, underground and surface waters).

Contamination by PTE and NORM currently represents one of the most sensitive problems for human health, due to their toxicity and radiological effects (Bonotto, 2015; Tchounwou et al., 2012).

Several types of cancers (e.g., breast, lung, skin, stomach, etc.), kidney damage, behavioral disturbances in children, among other health disorders, have been associated with short and long-term exposure to these pollutants (Järup, 2003). Although these adverse health effects have been well known for a long time, exposure to these types of pollutants is increasing, mainly in less developed countries.

Mining has become one of the anthropogenic activities that most impacts the environment, mainly in developing countries (Akinci & Guven, 2019; Reyes et al., 2019). Mining activities produce a huge quantity of wastes that predominantly contain PTE as by-products (Wang et al., 2019). The diffusion of these pollutants into the environment by natural factors or accidental release may cause long-term multi-elemental contamination of the entire ecosystem (Ling et al., 2019). Several works focusing on mining impacts on the environment indicate that mining areas can be considered extremely vulnerable regions to metal pollution and, consequently, to environmental degradation.

Brazil is one of the leading countries in mining, which on average represents 14.5% of total exports and 3.7% of gross domestic product (GDP) of the country (IBRAM, 2020). The state of Bahia (Northeast Brazil) is among the federal states with the most important and diverse mineral deposits (amethyst, chromium, gold, iron, manganese, nickel, vanadium and uranium). This fact has contributed to accelerated development and expansion of mining in this state.

However, most mining areas are in semiarid regions, where soils are poorly developed and suffer a lot of erosion due to climatic conditions. Therefore, prolonged mining activity makes it difficult to find another land use, once the mine is closed (Van Zyl and Straskraba, 1999).

In recent years, Brazil has been the scene of major mining accidents, which have been considered among the largest environmental disasters in the world mining industry (Burritt & Christ, 2018; WISE, 2020). Contrary to expectations, the government reduced resources for regulatory agencies and there was a setback in environmental legislation, thus placing the population living in mining areas in a situation of greater vulnerability (Do Carmo et al., 2017). In this context, studies carried out by public universities play an important role in the monitoring and evaluation of the possible impacts of mining activities, especially in inhabited areas. This is precisely the aim of the present work, which constitutes a precedent because it is the first time such a comprehensive investigation has been carried out in this region, characterized by a strong presence of mining operations and accelerated population growth.

In this study, the concentrations of thirty-four elements in natural, agricultural, and urban soils were determined in three important mining areas of the state of Bahia (NE-Brazil). This purpose was achieved by combining two of the most powerful analytical techniques: INAA and ICP OES. To assess the state of contamination in the topsoil, never before done in this region, different pollution indices were calculated. Robust statistical analyses were used to establish inter-element relationships and identify whether the elements have geogenic and/or anthropogenic origins, providing vital information on the local impacts of mining and other anthropogenic activities. All the data reported in this work can be used as environmental reference information in studies related to mining activities worldwide or as baseline values for future work in the same area.

## Study area

The study was conducted in three important mining areas: the iron and uranium mines in Caetité and the vanadium mine in Maracás. Both municipalities are

located in the semiarid region of the state of Bahia, northeast of Brazil (Fig. 1).

The municipality of Caetité, located in the central-southern region of Bahia, is 645 km away from Salvador (main city of the state). This region hosts several uranium-enriched zones and comprises the most important uranium province in Brazil, with a total reserve of ca.112,000 metric tons of triuranium octoxide ( $U_3O_8$ ) (Lobato et al., 2015). For this reason, this municipality concentrates—since 1999—the exploitation of this mineral by having the only active uranium mine (open-pit mine, area: 1700 ha) not only in Brazil but also throughout Latin America (INB, 2020). Roughly 300 tons per year of  $U_3O_8$  are produced from the orebodies located at the northern region of the municipality (Lobato et al., 2015). Furthermore, in 2005 an important iron ore field, with deposits that contain more than 10 billion tons of iron, was found in the southern part of the municipality (CETEM, 2013). This mine has the capability of producing up to 20 million tons of iron ore per year, which would place Bahia as the third iron-producing state in the country. (BAMIN, 2016).

The municipality of Maracás is located in the east-central region, 365 km from Salvador. The region boasts one of the highest-grade vanadium resources in the world with a total reserve estimated in 19,010 kt (Largo Resources, 2020). The mining activity began in 2014, and the mine (open pit, area: 17,690 ha) was projected to produce more than 10,000 tons of vanadium pentoxide ( $V_2O_5$ ) annually. The annual  $V_2O_5$  production guidance for 2020 was: 11,750–12,250 tons (Largo Resources, 2020).

The climate is semiarid characterized by an average annual temperature of 22 °C but can reach up to 35 °C during the summer season (December–February). The average precipitation is about 71.8 mm in Caetité, a little less in Maracás (67.0 mm). The rain events are erratic and are mainly concentrated during the summer. The winds generally blow from east and southeast and are particularly intense in the Caetité region (up to 15.3 km h<sup>-1</sup>).

Regarding geological features, the area is part of the São Francisco Craton. The Caetité region, specifically, is in the “Lagoa Real” lithological unit, which is a granite–gneissic complex. It covers an area of more than 2000 km<sup>2</sup> and crosses the area with N-S orientation (Pascholati et al., 2003). The pre-Espinhaço lithological unit, also with N-S orientation, dominates

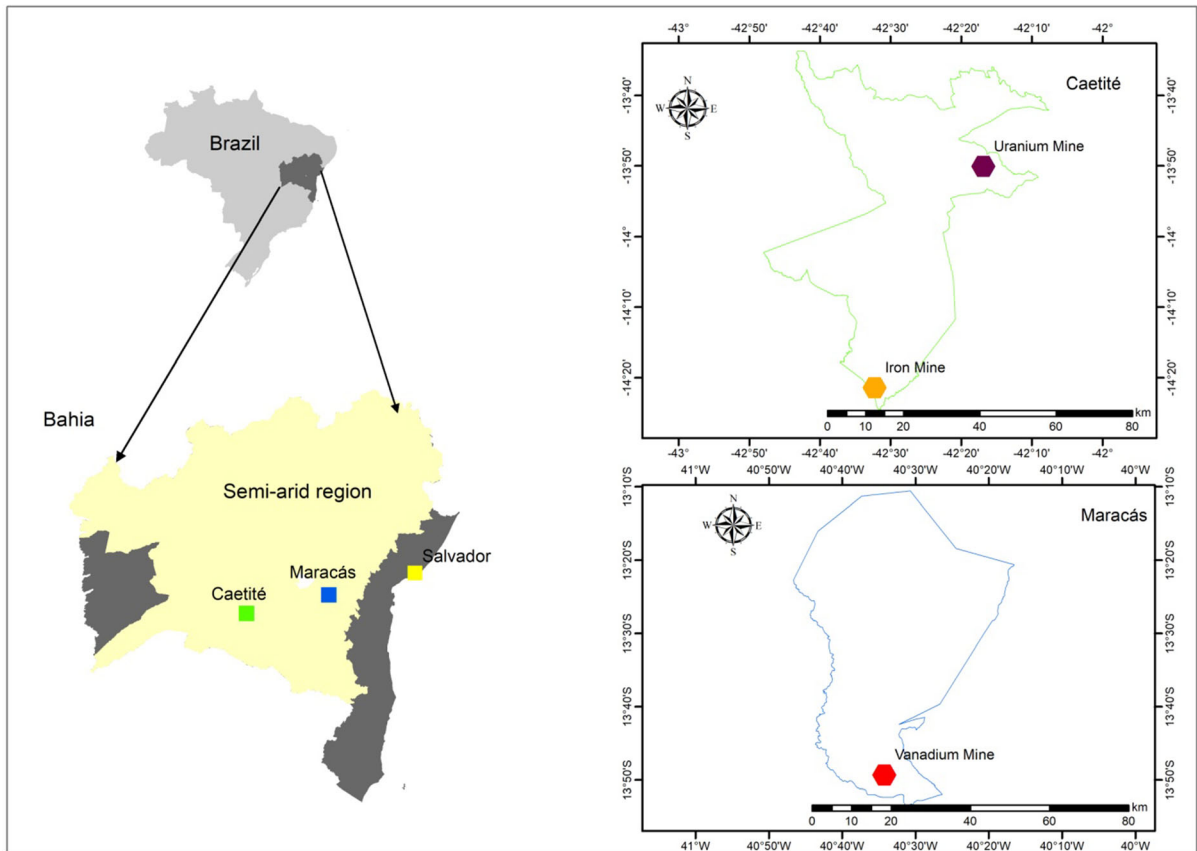


**Fig. 1** Geolocation of the municipalities of Caetité and Maracás, and the mining facilities studied in the state of Bahia (Northeast, Brazil). Yellow area corresponds to the semi-arid region (75% of the state territory)

the Maracás area. This unit is characterized by intense and complex folding and the presence of longitudinal faults (De Paula & Abrahão, 1991). In general, these lithological units are composed of alkaline granite bodies, orthogneiss, albites, and amphibolites rocks, among others. A heterogeneous relief predominates over the region with an altitude that varies between 800 and 1000 m and isolated mountains.

The predominant soil types are the dystrophic red-yellow latosols, eutrophic cambisols, and neosols (arenosols), the latter extremely susceptible to erosive processes. Previous work done in the region showed that latosols have a high permeability (percolation  $150 \text{ mm h}^{-1}$ ), while the cambisols have a moderate permeability (percolation  $5\text{--}150 \text{ mm h}^{-1}$ ) (PLANARQ, 1997). The study area is close to the two main hydrographic basins of the state of Bahia: the São Francisco and the Contas river basins. However, the

rivers of the region are ephemeral and remain dry most of the year, except during the rainy season.

In the neighborhood of the mining areas are located important urban centers. Approximately 80,000 people are considered to live near these mining areas. Agriculture and livestock are, in addition to mining, the most important economic activities in the region.

## Materials and methods

Since this section is vital for a clear understanding of the work, the main methodological steps are summarized in a flowchart presented in the Supporting Material (Figure S1).

Sampling procedure and sample preparation

In the three mining areas, natural soils were collected near the mining waste deposits. In the Maracás region, specifically, the sampling was carried out by contouring the margins of the Jacaré and Contas rivers, due to their proximity to the vanadium mine. In this case, the soil samples were collected 20–25 m away from the river banks. In the main human settlements around the mines, urban and agricultural soil samples were collected specifically in industrial, residential, and farming areas. A digital Global Positioning System (GPS) device was used to record the geographic coordinates at each sampling site (see Table S1). A total of thirty-four locations were sampled (Fig. 2): uranium mining area (UMA;  $n = 17$ ), iron mining area (IMA;  $n = 5$ ), and vanadium mining area (VMA;  $n = 12$ ).

The sampling procedure was performed based on the guidelines established by the US Environmental

Protection Agency (USEPA, 1989a) and the Brazilian Agricultural Research Corporation (EMBRAPA, 2014). After removing stones, thick materials, and other debris, topsoil samples (A horizon) were collected at a depth of 20 cm from the surface layer. In a  $5 \times 5$  m area, five individual samples were randomly collected, which were then pooled and homogenized to form a composite sample of 1 kg approximately. Finally, the composite samples were stored in sealed plastic bags, previously labeled and transported to the laboratory for further treatments and analyses.

The soil samples were dried in an oven at  $80 (\pm 2)$  °C until they reached a constant weight and then ground using a porcelain mortar and pestle to reduce the grain size to a fine powder. Afterward, the samples were sieved with a 150-mesh sieve ( $< 125 \mu\text{m}$ ). For both compositional analyses, representative subsamples of approximately 10 g of each sieved soil were taken and placed in 50-mL Falcon tubes, which were

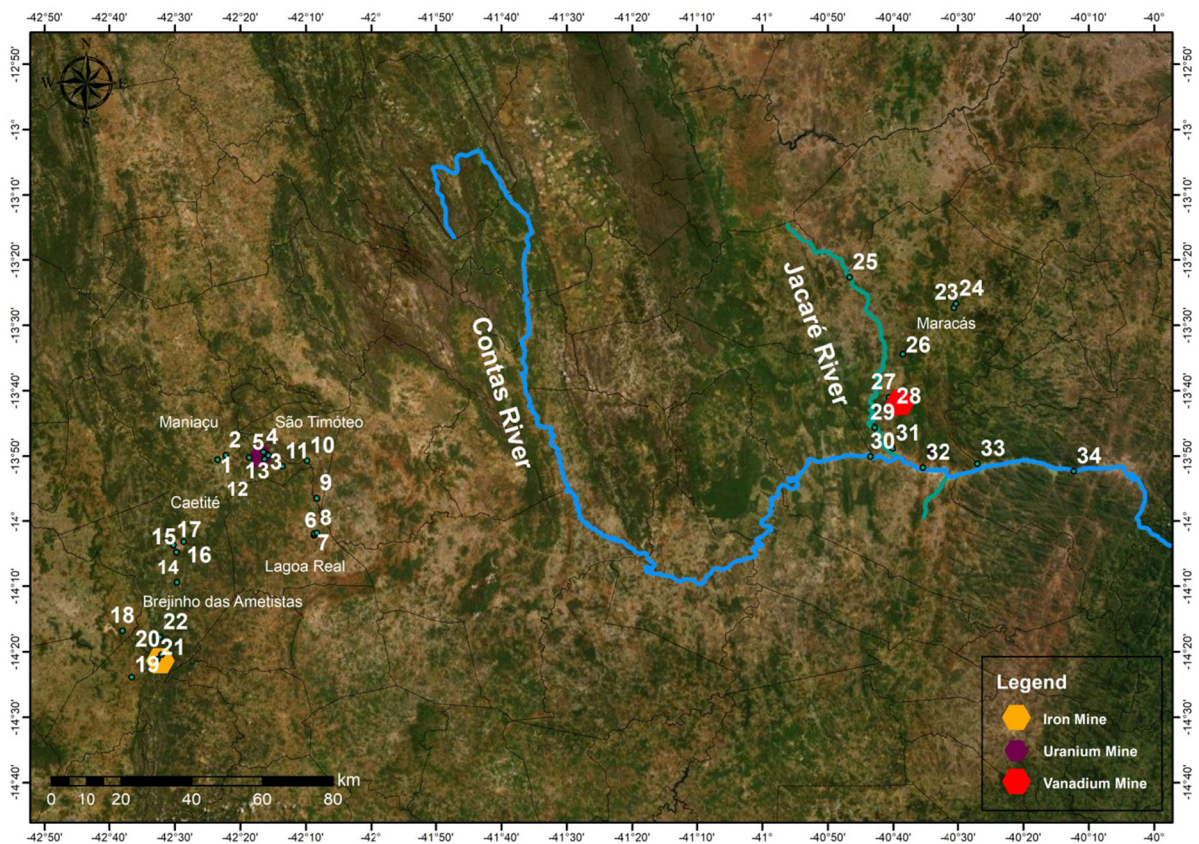


**Fig. 2** Map of the studied area and sampling sites

previously washed with an acid solution and then rinsed with deionized water.

### Instrumental neutron activation analysis (INAA)

This analysis was carried out at the research reactor IEA-R1 of the Nuclear and Energy Research Institute (IPEN), São Paulo, Brazil. The IEA-R1 is a pool type research reactor operating between 2 and 3.5 MW (IPEN, 2020).

For the sample analysis, five certified reference materials (CRMs) were used: BE-N (basalt),<sup>1</sup> GS-N (granite)<sup>2</sup>, JB-1 (basalt)<sup>2</sup> (see footnote 2), IAEA-Soil-7 (soil),<sup>3</sup> and W1 (diabase).<sup>4</sup> This set of geological CRMs was chosen because: they have a matrix similar to the samples analyzed and they exhibited the most precise concentration values for the elements of interest. These CRMs were irradiated and measured under the same conditions, together with the samples under study.

To determine the short-lived radionuclides of Al, Dy, Mn, Ti, and V, short-time irradiations were performed. Soil and CRM W1 samples ( $m \sim 78.5 \pm 0.5$  mg) were packed into sealed bags (1 cm x 1 cm), placed into a cylindrical polyethylene vial (called “rabbit”) and irradiated for 10 s in the reactor with the help of a pneumatic facility. The irradiated samples were measured twice (after 1-min and 1-h decay) using an HPGe coaxial detector (Canberra model: *GC2018*, Relative efficiency: 20%, Resolution: 1.8 keV). At the first count, the CRM and the soil samples were measured at 5 cm from the surface of the detector for 2 and 5 min, respectively. For the second count, they were placed in close-geometry configuration and measured for 10 min.

The long-lived radionuclides of As, Ba, Br, Ce, Co, Cr, Cs, Eu, Fe, Hf, K, La, Lu, Na, Nd, Rb, Sc, Sm, Ta, Tb, Th, U, Yb, Zn, and Zr were determined by exposing the samples to long-term irradiations. In this case, soil and CRMs (BE-N, GS-N, and Soil-7)

samples ( $m \sim 108.5 \pm 0.5$  mg) were separated into four different groups. Each group were packed in a column, wrapped in aluminum foil and then placed into an aluminum “rabbit.” The irradiation time ( $t_i$ ) for all groups was 8 h and before measuring the samples, it was necessary to wait for a “cool down” time ( $t_d$ ) until the permitted dose levels were reached. Some complementary technical information of this analysis is shown in Table S2 (Supplementary Material).

Long-time irradiated samples were measured in gamma-ray spectrometers, composed of HPGe coaxial detectors (Canberra model: *GX2020*, Relative efficiency: 20%, Resolution: 2.0 keV). The counting procedure was performed twice: after 6–7 days from irradiation (at 5 cm from the surface of the detector) and after 15–20 days from irradiation (in close-geometry configuration). In all cases, the measurement time was 1 h. The GENIE 2000 and S100 software were used for the acquisition and analysis of gamma-ray spectra.

The CAX program (Zahn et al., 2019) was used to calculate the elementary concentrations, their uncertainties and detection limits. This program uses the INAA relative method, which can be expressed mathematically as:

$$c_s = c_{CRM} \frac{N_\gamma^s \cdot m_{CRM}}{N_\gamma^{CRM} \cdot m_s} \cdot e^{\lambda(t_s - t_{CRM})} \quad [mg \text{ kg}^{-1}] \quad (1)$$

where  $m$  [kg] represents the irradiated mass of the soil and the CRMs samples,  $c$  [ $mg \text{ kg}^{-1}$ ] the concentration of the element of interest reported in the CRM datasheet, and  $N_\gamma$  [photons  $s^{-1}$ ] the gamma-ray count rate at the full-energy peak of energy  $E$ . The exponential term is introduced to take into account the time elapsed between the measurement of the soil samples and the CRM, and  $\lambda$  [ $s^{-1}$ ] is the decay constant of the specific radionuclide.

The uncertainties in the determined concentration values were up to 10%, except in some cases where the concentrations of some elements were below or near the limit of quantification (LOQ), determined by the Currie method (De Geer, 2004). Table S3 (Supporting Material) shows the main nuclear parameters of the radionuclides measured by INAA, as well as the LOQ for each element.

The quality of the measurement was established by determining the concentration of the elements of

<sup>1</sup> Certified Reference Material from Service d'Analyse des Roches et des Minéraux (SARM), France.

<sup>2</sup> Certified Reference Material from the Geological Survey of Japan (GSJ), Japan.

<sup>3</sup> Certified Reference Material from the International Atomic Energy Agency (IAEA), Austria.

<sup>4</sup> Certified Reference Material from the United States Geological Survey (USGS), United States.

interest in the CRM JB-1 and in mono-elemental references of Al, Mn, Ti, and V. The Z-score test was used to compare the concentration values obtained with those reported for the CRM. The Z-score values were not only within the accepted range  $[-2, 2]$  but also 90% of the values were within  $[-1, 1]$ , which constitutes evidence of the good accuracy of the results (see Fig. S2). The fact that Br concentration was reported as a “provisional value” in CRM JB-1 and the lack of a mono-elemental reference of Dy prevented both elements from being included in the quality control test. However, they were considered in the analysis based on the high level of coincidence obtained for the other elements.

#### Inductively coupled plasma optical emission spectrometry (ICP OES)

Since the isotopes frequently used in the INAA to determine Cd, Cu, Ni, and Pb present some difficulties such as low isotopic abundance, small or null neutron capture cross sections, and low gamma-ray branching ratios; these four elements were determined by ICP OES. In this case, a subsample of  $250.0 (\pm 0.1)$  mg of each sieved soil was placed in a tube, and 2.5 mL of concentrated nitric acid ( $\text{HNO}_3$ ) and 1.5 mL of 37% hydrochloric acid (HCl) were added with a pipette. *Aqua regia* digestion, which is a standardized method for analyzing metals in environmental samples, was performed following the procedure recommended by ISO 11466 (1995). This procedure was carried out using a TECNAL digester block (TE-007 MP) with a cold finger. The acid solution was heated at  $130 (\pm 2)$  °C for 5 h, then cooled to room temperature and finally centrifuged at 2000 rpm for 5 min. Once the acid digestion procedure was completed, the samples were transferred to clean 50-mL Falcon tubes and Milli-Q ultrapure water (resistivity:  $18.2 \text{ M}\Omega \text{ cm}^{-1}$ ) was added to complete 15 mL.

Digested soil samples were analyzed using the spectrometer (ICP OES, Varian 710-ES) operated under the following conditions: RF power (1.3 kW), plasma gas (Argon), plasma gas flow ( $15 \text{ L min}^{-1}$ ), auxiliary gas flow ( $1.5 \text{ L min}^{-1}$ ), nebulizer pressure (150 kPa), nebulizer gas flow ( $0.7 \text{ L min}^{-1}$ ), stabilization time (15 s). Each sample was analyzed in triplicates for 3 min each.

The calibration of the equipment was carried out before the measurements of the samples by using

multi-elemental high-purity standards (South Carolina, USA) and mono-elemental Merck standards (Darmstadt, Germany). To determine the limit of quantification, ten blank samples were prepared using 15 mL of Milli-Q ultrapure water and then measured at the same operating conditions. The spectral lines and the LOQ (calculated as in, IUPAC, 1978) of the analyzed elements (Cd, Cu, Ni, and Pb) are exhibited in the supporting material (see Table S4).

Although the *aqua regia* digestion gives the pseudo-total concentration, the recovery percentages of the selected elements obtained from the CRM analysis were higher than 86%. Furthermore, the calculated Z-score values were between 0.2 and 0.8 (Fig. S1), thus indicating that the adopted procedure leads to reliable results.

#### Assessment methods of contamination in soils

In order to assess quantitatively the state of soil contamination in the studied areas, single and combined indices of pollution were calculated. These indices allowed us to classify the areas in various levels of contamination according to the metal content. Since the indices used in this work have been widely discussed in many scientific articles, the equations and parameters involved in the calculation of each index were summarized in Table S5 (Supplementary Material).

Two single indices, the enrichment and the contamination factors (EF and CF) were calculated to identify the pollution level for each individual metal. They are commonly used to estimate the degree of intensity of the anthropogenic impact on soils (Hadzi et al., 2019). The EF calculations were performed using Al as the reference element, which is usually chosen because it is one of the most common elements in the Earth's crust (Bern et al., 2019).

Additionally, the combined indices: modified degree of contamination ( $\text{mC}_d$ ), Pollution Load Index (PLI), and Pollution Index for Rare Earth Elements (REEP) were calculated to assess the level of contamination by considering the simultaneous presence of numerous pollutants. The  $\text{mC}_d$  and PLI both calculated from the CF are widely used in environmental studies to identify the levels of metal pollution accumulation (Fosu-Mensah et al., 2018), whereas the REEP is specifically defined for assessing the level of

contamination due to the content of rare earth elements in a region of interest (Jinxia et al., 2010).

Table 1 shows the different contamination categories for all the indices used in this study, except for PLI, which has only three categories:  $PLI < 1$  indicates no contaminated,  $PLI = 1$  (base line of pollution), and  $PLI > 1$  contaminated (Tomlinson et al., 1980).

Due to the fact that background values play an important role in the correct interpretation of geochemical data and in accurately assessing the level of contamination; they must be chosen carefully. In this study, the background values for 19 of the 34 elements determined were taken from Machado (2018), whose work focused on the “Lagoa Real” lithological unit. However, in that study the values of elements of interest such as As, Cd, Co, Cr, Cu, Mn, Ni, Pb, and Zn were not reported. For that reason, the values reported by Da Silva et al. (2015) and Biondi et al. (2011) were used as reference concentrations for those elements. These studies established background values for a semiarid region, also located in northeastern Brazil, with similar geological and climatic characteristics to that of our study.

In the case of Br, Cs, Hf, Ta, and V for which there are no previous studies in the region that report their background concentrations, the values of the Upper Continental Crust (UCC), reported by Rudnick and Gao (2014), were used only for comparative purposes. Likewise, the concentrations obtained for REE and Sc were compared with the value reported by De Sá Paye et al. (2016), who investigated the distribution of these elements in 88 sites distributed across Brazil. Finally, it is worth mentioning that Table S6 summarizes all the background values used in this work, as well as the guideline values for agricultural and urban soils established by Brazilian legislation (CONAMA 420/2009) and the USEPA (2020).

## Data statistical analysis

All data obtained were statistically analyzed using the STATISTICA v18.0 software. Each metal concentration data set was evaluated in terms of descriptive statistical parameters, such as minimum and maximum values, median, mean, mean standard deviation (M.S.D), skewness, and kurtosis. The assumption on data normality distribution was evaluated by the Kolmogorov–Smirnov test at a level of significance  $p < 0.05$ .

To identify relationships between the elements, Spearman correlation coefficients ( $r_s$ ) were computed. The Spearman test provides a statistical measure of the strength of a monotonic relationship between paired data. Unlike Pearson’s correlation, this nonparametric test does not require that the data follow a normal distribution. The principal component analysis (PCA) and hierarchical cluster analysis (HCA) were used to identify patterns in the distribution of metal throughout the region. These multivariate statistical tools have been used successfully in environmental pollution studies (Hadzi et al., 2019; Reyes et al., 2019). Prior to the calculation of the PCA, concentration data were standardized and subjected to a centered log-ratio (clr) transformation as shown in Bern et al. (2019):

$$\text{clr}(C_X) = \log_{10} \left( \frac{C_X}{\sqrt[n]{C_1 \cdot C_2 \cdot \dots \cdot C_n}} \right) \quad (2)$$

where the log-ratio is applied to the concentration of individual elements ( $C_X$ ) after dividing by the geometric mean of a particular subset of all element concentration for a given sample. This transformation is commonly used for the analysis of compositional data (CoDA).

**Table 1** Soil pollution categories based on the calculated indices (CF, EF,  $mC_d$ , and REEP)

Contamination level	CF*	EF*	$mC_d$ *	REEP**
Unpolluted	< 1	< 1	< 1.5	≤ 0.5
Low to moderately polluted	–	1–3	1.5–2	0.5–1
Moderately polluted	1–3	3–5	2–4	1–2
Moderately to heavily polluted	–	5–10	4–8	–
Heavily polluted	3–6	10–25	8–16	2–10
Heavily to extremely polluted	–	25–50	16–32	–
Extremely polluted	≥ 6	≥ 50	≥ 32	> 10

\*Lower limit of the interval is included: [].

\*\*Upper limit of the interval is included: ()

## Results and discussion

To carry out a more detailed analysis of the data obtained, the thirty-four measured elements were divided into six groups: This classification was done following chemical, geological and toxicological criteria such as the ratio of charge and ionic radius, abundance in the Earth's crust, and toxicological effects in living organisms. Tables S7–S9 summarize the descriptive statistic of all the elements in each mining region.

Crustal rock forming elements (CRFE): Al, Fe, K, and Na

CRFE together with Ca and Si constitute the predominant minerals in the Earth's mantle, which makes them the most abundant elements in soils (Railsback, 2003). In the three mining areas, the highest concentration value was observed for Al (IMA = 8.7%, UMA = 11.6% and VMA = 9.2%). The IMA region presented the highest Fe concentration (7.4%), being the soil sample (SL-20) the one that exhibited the maximum value (18.7%). These were expected results, considering that hematite [ $\text{Fe}_2\text{O}_3$ ] and itabirite (banded-quartz hematite) are the main minerals in this region and both have high Fe contents: 66% and 32%, respectively (ENRC, 2012). Regarding the K content, the samples showed high variability, which reached up to 40% in the urban area of Caetité. Na concentrations exhibited values did not exceed 2.6%, which is typical of saline and sodic soils found in semiarid regions.

According to the Kolmogorov–Smirnov test, in IMA only Al showed a normal distribution ( $p < 0.05$ ), whereas Fe, K, and Na exhibited right-skewed and leptokurtic distributions. In UMA, only K and Na did not follow a normal distribution, and in VMA all the elements are normally distributed.

Forty-four percent of the soil samples presented a low to moderate enrichment level of Fe ( $1 \leq \text{EF} < 3$ ) and only the samples collected at iron (SL-20) and vanadium (SL-28) mines exhibited a moderate enrichment ( $3 \leq \text{EF} < 5$ ). Eighteen percent of the samples showed low to moderate K enrichment, most of them corresponding to urban soils or close to mining areas. In the case of Na, EF values showed a low enrichment for this metal. The average contamination factors revealed that in the three mining areas there is a moderate pollution of Al and Fe ( $1 \leq \text{CF} < 3$ ). In fact,

Al concentration in all urban soils exceeded 7.7%, the reference value for urban soils recommended by the USEPA (2020). Likewise, the soil in the urban area of Caetité (SL-15 and SL-16) presented Fe concentrations above the reference value (5.5%). Most agricultural soils showed moderate pollution of Al, Fe, and K. The higher values of  $\text{mC}_d$  and PLI were observed in SL-03 ( $\text{mC}_d = 1.6$ ;  $\text{PLI} = 1.6$ ), SL-13 ( $\text{mC}_d = 1.7$ ;  $\text{PLI} = 2.1$ ), and SL-20 ( $\text{mC}_d = 2.2$ ;  $\text{PLI} = 1.4$ ), which corresponds to the UMA and IMA waste areas. These results indicate that soils collected near the mines have been negatively impacted by this activity.

It has been pointed out that wastes from mining activities, specifically from uranium production, contain oxides of aluminum, iron, and potassium in high concentrations (23.4%, 3.9%, and 11.2%, respectively), which are easily transported in diluted form in the liquid effluents (Fernandes et al., 2004). For that reason, the eventual leaching of these effluents and/or diffusion by natural factors may explain the high concentrations of these elements observed in the soils around the mines.

Large-ion lithophile elements (LILE): Ba, Cs, and Rb

The term LILE refers to trace elements characterized by having large ionic radii; which are “incompatible” elements and generally end up enriched in the crust (Chauvel & Rudnick, 2016). The concentrations of Ba and Rb in the mining areas slightly exceeded ( $\sim 1.3$  times) the values reported for the UCC; however, they are lower than the reported background values, which suggests that the study region presents a natural enrichment of both elements. In UMA and VMA, Ba and Rb followed a normal distribution, while in IMA both elements exhibited positive skewness, so they follow asymmetric distributions.

More than 85% of the samples exhibited EF values below 1, reinforcing that Ba and Rb may have a crustal origin (Marrugo-Negrete et al., 2017). The CF values showed that 62% of the samples can be considered unpolluted by these elements ( $\text{CF} < 1$ ) and that only agricultural and urban soils exhibited a discrete contamination. Figure 3 shows that the concentration of Ba found in the regional agricultural and urban soils exceeds the values established by the Brazilian legislation for these soils.

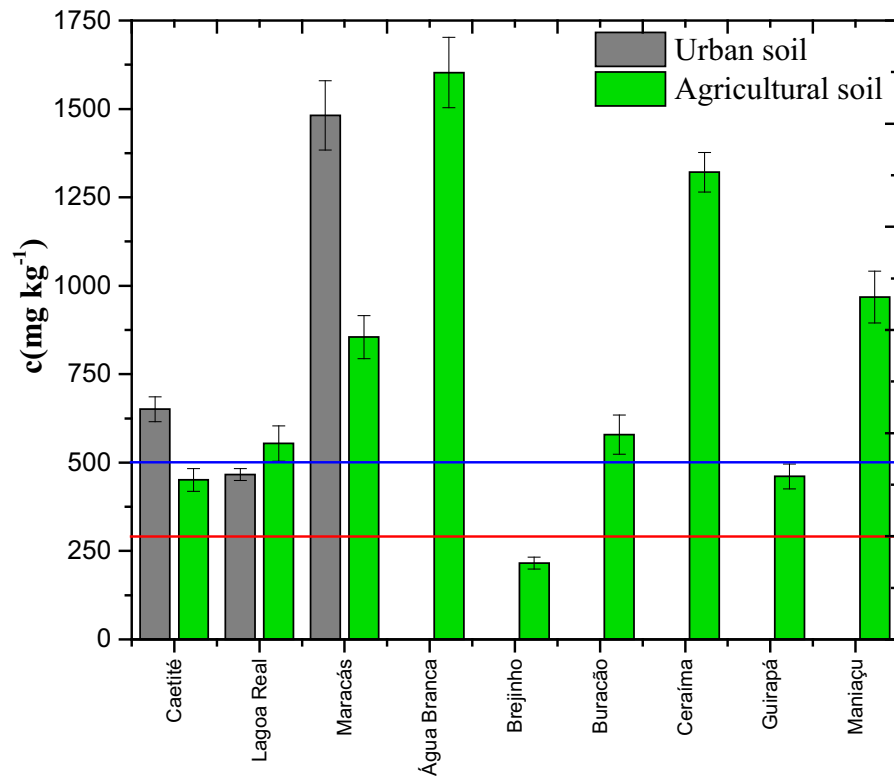


**Fig. 3** Concentration of Ba in the agricultural and urban soils collected in the main human settlement of the region of study. Solid lines represent the guideline values for agricultural soil

(red line: 300 mg kg<sup>-1</sup>) and urban soils (blue line: 500 mg kg<sup>-1</sup>) recommended by CONAMA, 2009

The values of Cs concentration presented high positive kurtosis (greater than five), suggesting it follows a leptokurtic distribution. The overall concentration (2.2 mg kg<sup>-1</sup>) was two times lower than the UCC value, indicating a depletion of this element. This result was corroborated by the Rb/Cs ratio obtained for the analyzed soils, which was 2.8 times the value reported for the UCC: 20 (Rudnick & Gao, 2014).

High field strength elements (HFSE): Hf, Ta, Ti, and Zr

The elements that make up this group have high ionic valencies compared to their radii and are considered to be “conservative” due to their limited mobility during geological processes (Jiang et al., 2005). In the three mining areas, HFSE concentrations in soils decreased in the following order: Ti > Zr > Hf > Ta. The Kolmogorov–Smirnov test confirmed that all data sets are distributed following a normal distribution.

Higher concentrations of Ti were obtained in the three regions, which was an expected result because titanium is the seventh most abundant element in the Earth’s crust. The IMA region exhibited the highest concentrations (8823 mg kg<sup>-1</sup>), which could be explained based on the association of Ti with iron ores (*e.g.*, ilmenite: FeTiO<sub>3</sub>) (Rudnick & Gao, 2014). However, Ti concentrations of up to 7.5 times the background value (2127 mg kg<sup>-1</sup>) suggest a predominantly anthropogenic origin, since the rocks of the studied region have regular content (2.26–7.53%) of titanite (CaTiSiO<sub>5</sub>) in their composition (Machado, 2008). Nowadays, Ti is added to asphalt, concrete, and commercial fertilizers; it is also used in paint pigments (titanium white: PW6) and in iron and vanadium alloys (Lyu et al., 2017).

Indeed, the CF values obtained for Ti reflect a significant pollution level, specifically in urban soils and near the iron and vanadium mines. In the Caetitê region (IMA and UMA), 46% of the samples showed heavy pollution (3 ≤ CF < 6) and 18% can be

classified as extremely polluted ( $CF \geq 6$ ). In VMA, the CF values ranged from 1.3 to 3.6, indicating a moderate to heavy pollution. The points SL-27 and SL-28, which are the closest to vanadium mine, exhibited the highest CF values in this region. The EF values for Ti revealed that 81% of the samples are moderately enriched ( $3 \leq EF < 5$ ).

The Hf, Ta, and Zr contents in soils showed a similar behavior throughout the region. The samples belonging to the UMA and VMA regions presented Hf, Ta, and Zr concentrations higher than the IMA values: 3, 1.5, and 4 times, respectively. Furthermore, the regional concentrations of these elements are 6, 3, and 7 times higher than the UCC values (Hf:  $5.3 \text{ mg kg}^{-1}$ , Ta:  $0.9 \text{ mg kg}^{-1}$ , Zr:  $193 \text{ mg kg}^{-1}$ ). The EF values revealed that 71% of the samples present a moderate enrichment of both Hf and Zr ( $3 \leq EF < 5$ ), while 10% exhibited moderate enrichment of Ta. Based on these findings, it can be stated that the region is naturally enriched in Hf, Ta, and Zr. However, the fact that the highest EF values for these elements were observed in the sample collected near the vanadium mine (SL-27), suggests that the enrichment levels may also be associated with the impact of the mining activities.

Naturally occurring radioactive material (NORM):  
Th and U

Across the region, Th concentrations ranged between  $2.6$  and  $62.7 \text{ mg kg}^{-1}$ , whereas U values varied from  $1.2$  to  $18.6 \text{ mg kg}^{-1}$ . The assumption of a normal distribution for both elements was corroborated by the Kolmogorov–Smirnov test. As expected, the concentrations were higher in the UMA; whereas the IMA had the lowest values (see Fig. 4). More than 60% of the samples exhibited Th and U contents above the geological reference values (Th:  $24.3 \text{ mg kg}^{-1}$ , U:  $3.1 \text{ mg kg}^{-1}$ ) reported by Machado (2008). In the study region, the Th/U ratio obtained was: 4.8, which is slightly higher than the reported for the UCC: 4.3 (Rudnick & Gao, 2014), but is still within the range of acceptable values.

The soil samples collected in the district of Maniaçu, the closest to uranium mine, showed an extreme contamination of U ( $CF \geq 6$ ) and it was the only place where the guideline value of U in urban soils ( $16 \text{ mg kg}^{-1}$ , USEPA (2020)) was exceeded. Natural soils around the uranium mine (SL-03 and SL-12) also

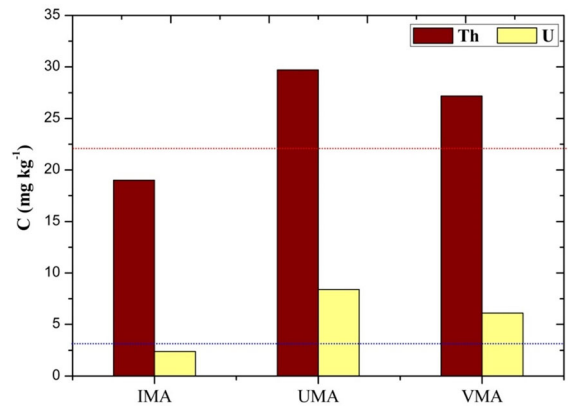


**Fig. 4** Concentrations of Th and U in each mining area. Dotted lines represent the geological reference values for Th:  $24.3 \text{ mg kg}^{-1}$  (red) and U:  $3.1 \text{ mg kg}^{-1}$  (blue) Machado (2008)

showed severe contamination ( $3 \leq CF < 6$ ). The average values of  $mC_d$  (2.2) and PLI (1.8) indicated a level of moderate contamination in UMA. On the other hand, in IMA the average value of the same indices ( $mC_d = 0.9$  and  $PLI = 0.7$ ) suggested that this area can be classified as uncontaminated concerning the Th and U content in soils. Finally, in the VMA region,  $mC_d$  and PLI values (1.6 and 1.5, respectively) revealed a low to moderate level of contamination. The soil sample SL-25 showed the highest EF values of Th (5.9) and U (7.5) in this area, indicating a moderate to severe enrichment for both elements. This sampling point, located north-east of Maracás, corresponds to an area of confluence of two geological blocks: Gavião and Jequié blocks. Precisely, in areas of geological contact high concentrations of Th and U are expected to occur (De Queiroz, 2016).

Although the whole region is an area naturally enriched with NORM, the impacts of mining activity on soils should not be neglected. It has been reported that Th and U can be found in the composition of the waste in the tailings dam with average concentrations of 0.004 and 0.018%, respectively (Fernandes et al., 2008). The diffusion of these elements in the environment can increase their concentrations in soils, thus becoming Technologically Enhanced Naturally Occurring Radioactive Materials (TENORM). Human health effects ranging from headaches, cataracts, congenital disorders, sterility to leukemia, and other types of cancer are directly associated with the presence of these radionuclides in the soil and water (IAEA, 2005).

Rare earth elements (REE): Ce, Dy, Eu, La, Lu, Nd, Sc, Sm, Tb, and Yb

Figure 5a shows the comparison between the concentrations of REE in the three mining areas and the values reported in similar studies. As can be seen, the concentrations of REE reported for the “Lagoa Real” lithological unit and those detected in the study areas are higher than the reported for Brazilian soils and the UCC, indicating a certain level of natural enrichment of these elements in the region. In the three mining areas, Ce, La, and Nd were the most abundant elements and their concentrations are up to four times higher than those reported for the UCC, but remain below the background values. Scandium was the only element that showed a concentration similar to the value reported for Brazilian soils and UCC.

For a better analysis, the REE were subdivided into light rare earth elements (LREE: La, Ce, Nd, Sm, Eu, Sc) and heavy rare earth elements (HREE: Tb, Dy, Yb, Lu). The LREE/HREE ratio in each region was: 26.4 (IMA), 21.0 (UMA), and 14.7 (VMA), which shows that LREE contents are significantly higher and that they account for 94% to 96% of the total REE content determined in soil samples. These percentage values are in agreement with the trend described in similar studies (De Sá Paye et al., 2016; Wang & Liang, 2015).

In IMA, the data set for Ce, Dy, Eu, La, Nd, and Sm showed high positive skewness values, indicating that these elements follow a distribution with a long right tail. In the other two mining areas, Kolmogorov–Smirnov test showed that all REE (except for Sc) are normally distributed. The positive skewness and kurtosis indicate that Sc follows a right-skewed and leptokurtic distribution.

The results of the sum of all REE ( $\Sigma$ REE) showed high contents of these elements throughout the study area (Fig. 5b). In 10 samples (29%), the background value ( $\Sigma$ REE<sub>BG</sub>) reported for the lithological unit “Lagoa Real” was exceeded, whereas 82% of the samples surpassed the  $\Sigma$ REE reference value for Brazilian soils: 176 mg kg<sup>-1</sup> (De Sá Paye et al., 2016). The samples belonging to UMA (from SL-01 to SL-17) and VMA (SL-23 to SL-34) exhibited higher concentrations of REE compared to IMA samples. However, the sample with the highest concentration: 1961 mg kg<sup>-1</sup> corresponds to the agricultural soil

(SL-18) collected in the district of Ceraíma in the IMA region.

The average values for EF ranged between 0.6 and 0.8, which confirms a low enrichment of REE in the region. However, some agricultural soils (SL-08, SL-11, SL-18, and SL-33) exhibited a discrete enrichment of REE ( $1 \leq EF < 3$ ). This behavior was observed for all REE, except Sc, which also showed discrete levels of enrichment but mostly in urban soils. Similar results revealed the CF analysis. Most of the samples (76%) presented a moderate level of contamination ( $1 \leq CF < 3$ ) by at least one of these elements, while 38% showed a moderate contamination by four or more elements. The agricultural soil collected in Ceraíma (SL-18) presented severe contamination ( $3 \leq CF < 5$ ) for all the LREE.

To have an overview of the state of contamination by REE, the combined indices  $mC_d$ , PLI, and REEP were calculated. Based on the average values of these indices ( $mC_d = 0.9$ , PLI = 0.8, and REEP = -0.1), mining areas can be classified as unpolluted due to the content of REE in soils. The specific values for each mining area are summarized in Table S10 (Supporting Material).

Although REE seem to have a natural origin, it is worth mentioning that agriculture and mining are considered two main causes for increasing the concentration of REE in soils (De Sá Paye et al., 2016). The use of REE-based fertilizer would explain the high concentrations detected in agricultural soils. In the environmental laws consulted for this study, only a reference value for La was found for urban soils: 3.9 mg kg<sup>-1</sup> established by USEPA (2020). This value was exceeded in all analyzed urban soils. Unfortunately, the lack of recommended guideline values for REE did not allow further analysis of soil contamination. The existence of reference values is a crucial aspect, especially for agricultural soils, because high concentrations of REE could lead to changes in soil properties and fertility, and can reduce the diversity of soil macrofauna (Jinxia et al., 2010).

Potentially toxic elements (PTE): As, Br, Cd, Co, Cr, Cu, Mn, Ni, Pb, V, and Zn

Although these are not the only elements analyzed that may be harmful due to their toxicological potential, it was decided to form this specific group because these elements are the most researched and widely discussed

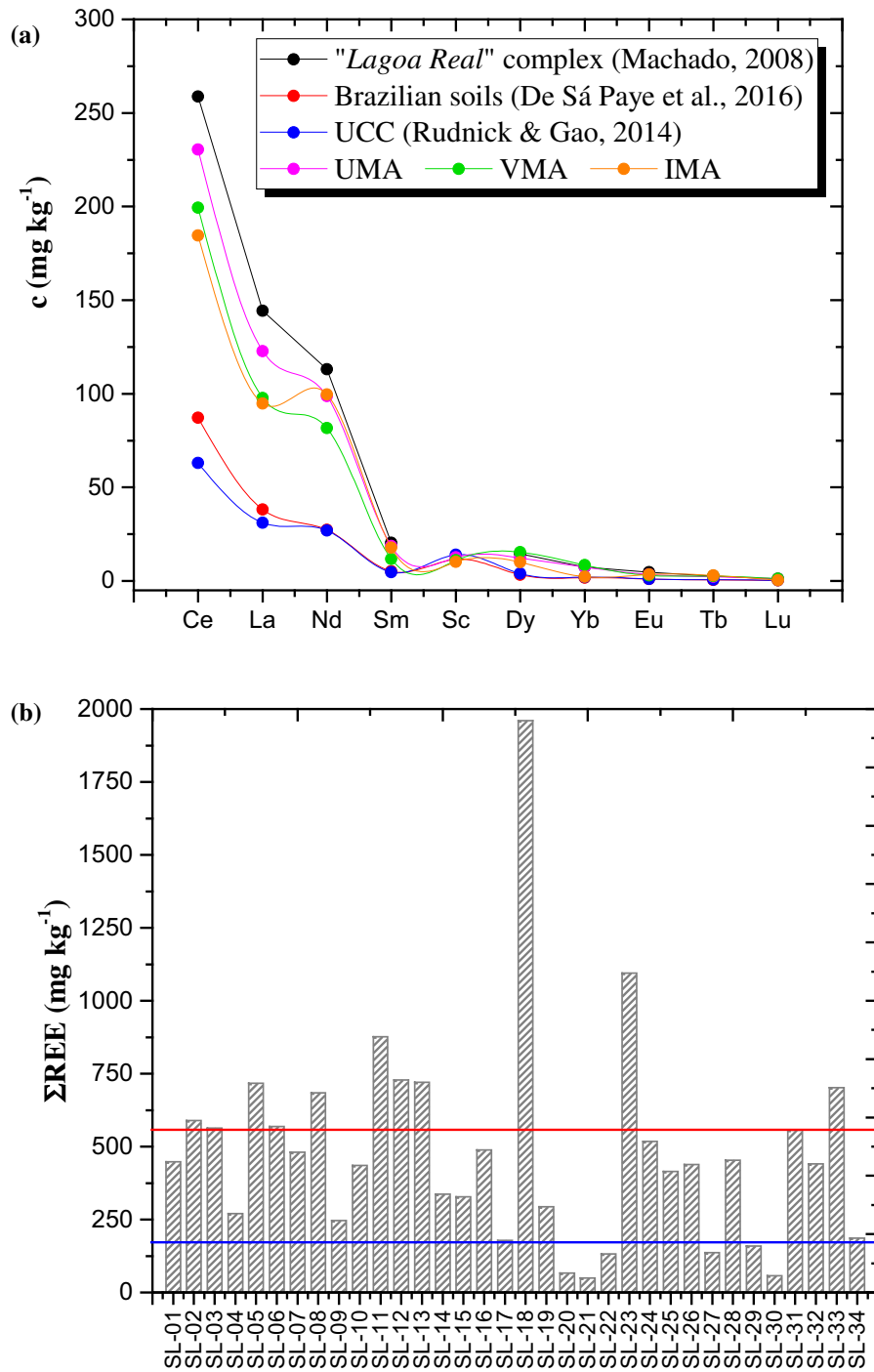


**Fig. 5** a) Average concentrations of REE in the mining areas and those reported for “Lagoa Real” lithological unit (Machado, 2008), Brazilian soils (De Sá Paye et al., 2016) and Upper Continental Crust (UCC) (Rudnick & Gao, 2014). b) Sum of

total REE (ΣREE) in soil samples. The solid line indicates the reference value for Brazilian soils (blue line: 176 mg kg<sup>-1</sup>, De Sá Paye et al., 2016) and for “Lagoa Real” lithological unit (yellow line: 565 mg kg<sup>-1</sup>, Machado, 2008)

in environmental pollution studies. The term “heavy metals,” commonly used in this type of studies, was avoided because it is generally used to refer to transition metals and/or semimetals, but does not include highly toxic nonmetallic elements as Br.

In IMA the average concentrations of PTE in the soil decreased in the following order:  $Mn > V > Cr > Ni > Zn > As > Cu > Pb > Co > Br > Cd$ , and only the As, Cr, Cu, Pb, V, and Zn showed a normal distribution according to the Kolmogorov–Smirnov test. The other elements presented positive skewness values, thus indicating right-tail asymmetric distributions. In UMA, Zn ranked second with a concentration of  $99 \text{ mg kg}^{-1}$ , which is twice as high as that observed in the other mining areas. In addition, V and Cr fell two positions and As occupied the last position. The elements As, Br, Cr, Cu, Pb, and V presented right-skewed distributions and the high kurtosis value observed for Pb (12.04) showed that most of the data is clustered about the central value. Finally, in VMA the soils exhibited the highest values of V ( $111 \text{ mg kg}^{-1}$ ) and Pb ( $12 \text{ mg kg}^{-1}$ ), occupying the second and fifth positions, correspondingly. In this region, Cd concentrations were below the LOQ in all the samples. The application of the Kolmogorov–Smirnov test revealed that only As, Mn, Pb, and Zn are normally distributed.

Natural soils around the iron mine (SL-20 to SL-22) showed concentrations of As, Cd, Cr, and Ni above the prevention values for these elements: As ( $15 \text{ mg kg}^{-1}$ ), Cd ( $1.3 \text{ mg kg}^{-1}$ ), Cr ( $75 \text{ mg kg}^{-1}$ ), and Ni ( $30 \text{ mg kg}^{-1}$ ) established by the Brazilian legislation (CONAMA, 2009). Likewise, the soil sample collected near the vanadium mine (SL-28) exhibited concentrations of Cr and Ni higher than the CONAMA guideline. All the natural soils in UMA presented Cd concentrations that exceeded the prevention value, and two of them (SL-04 and SL-06) also showed Ni concentrations above the limit. In the case of agricultural and urban soils, Ni was the only element found in concentrations above the limit values recommended by the CONAMA (2009) for these types of soils.

The range of contamination factors (CF) for the different elements was: 0.5–21 (As), 7.2–38 (Cd), 0.1–20 (Co), 0.5–10 (Cr), 0.1–5.1 (Cu), 0.2–11 (Mn), 0.1–37 (Ni), 0.1–1.7 (Pb), and 0.1–5.0 (Zn). The box plot shows the distribution of the CF for these elements (Fig. 6). As can be noticed, all the elements,

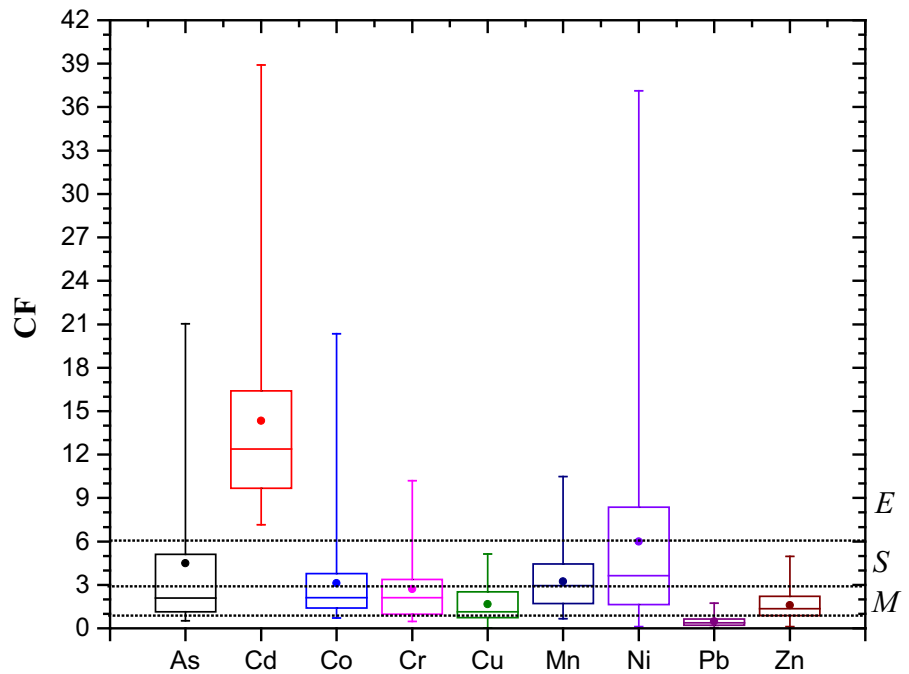
except for Pb, have average CF values higher than the unity, which warns of a certain level of contamination by these metals in the soils of the region. The average values of CF revealed a moderate level of contamination of Cr, Cu, and Zn ( $1 \leq CF < 3$ ); severe contamination of As, Co, Mn, and Ni ( $3 \leq CF < 6$ ); and an extreme degree of contamination of Cd ( $CF \geq 6$ ).

The  $mC_d$  and PLI indices showed that IMA and UMA are the most polluted regions based on PTE content. More than 60% of the samples collected in the municipality of Caetité, which includes both iron and uranium mines, exhibited a moderate to severe contamination level ( $4 \leq mC_d < 8$ ). Likewise, all samples except SL-09 presented PLI values greater than one, thus corroborating the level of contamination of the soils. In the VMA, only the sample near the vanadium mine (SL-28) showed a severe pollution level.

The regional average EF values suggest a low enrichment of Pb ( $EF < 1$ ), a low to moderate enrichment of Cr, Cu, Mn, and Zn ( $1 \leq EF < 3$ ), a moderate enrichment of As, Co, and Ni ( $3 \leq EF < 5$ ), and a severe enrichment of Cd ( $10 \leq EF < 25$ ). The soils collected near the iron mine (SL-20, SL-21, and SL-22) showed severe enrichment of As and Cd, thus indicating that the presence of these pollutants is considered non-crustal, *i.e.*, they have an anthropogenic origin, mainly related to iron mining activities. Likewise, most of the agricultural soils exhibited moderate enrichment of As, Cd, and Mn. Severe enrichments of Co and Mn were observed in the soil sample collected near the vanadium mine (SL-28). At this location, the V concentration detected ( $412 \text{ mg kg}^{-1}$ ) is 4.2 times higher than the UCC value, evidencing the enrichment of this metal in this mining area, as expected. In the case of urban soils, a moderate to severe enrichment of Cd, Cr, Cu, and Ni was observed. In addition, Br concentrations up to 11 times higher than the UCC value were also observed in urban soils.

Given that most PTEs are generally produced by human activities (Marrugo-Negrete et al., 2017), the levels of enrichment and pollution detected in the region reflect the impacts on the quality of the soils of different anthropogenic activities such as mining, agriculture, as well as industrial and domestic emissions, among others.

**Fig. 6** The box and whiskers plots show the distribution of the Contamination Factor (CF). Boxes depict 25th, 50th (median), and 75th percentiles, while the whiskers indicate the minimum and maximum values. Average values (●). Dotted lines indicate the categories of CF: Moderate ( $1 \leq CF < 3$ ), Severe ( $3 \leq CF < 6$ ), Extreme ( $CF \geq 6$ )



Statistical analysis results and identification of pollution sources

Spearman correlation analysis was used to obtain information on similar pollution sources. In the UMA region, moderate positive correlations were observed for  $p < 0.05$  for Al–Fe ( $r_s = 0.63$ ), Al–K ( $r_s = 0.56$ ) and Fe–K ( $r_s = 0.64$ ). This trend was also observed in the other two mining regions, where there are also moderate correlations between Al and Na ( $r_s \sim 0.69$ ). Strong positive correlations were observed between Ba and Rb in the study region (IMA:  $r_s = 0.91$ , UMA:  $r_s = 0.88$ , and VMA:  $r_s = 0.80$  at  $p < 0.01$ ). Likewise, Ba and Rb were moderately correlated with Al ( $r_s \leq 0.62$ ,  $p < 0.01$ ) and very strongly with K ( $r_s \geq 0.90$ ,  $p < 0.01$ ). These interrelations can be explained based on the geological study conducted by Machado (2008). According to this work, albite [NaAlSi<sub>3</sub>O<sub>8</sub>], biotite [K (Mg,Fe)<sub>3</sub>AlSi<sub>3</sub>O<sub>10</sub> (F,OH)<sub>2</sub>], and feldspars rich in aluminum and iron oxides (~ 15% and 3–5%, respectively) are among the main minerals found in the granite–gneissic rocks. These feldspar minerals are responsible for Ba and Rb concentrations because celsian, hexacelsian [BaAl<sub>2</sub>Si<sub>2</sub>O<sub>8</sub>], and rubicline [(Rb,K)(AlSi<sub>3</sub>O<sub>8</sub>)] are also found in the granite–gneissic rocks in concentrations ranging from 5 to 18%.

Hafnium and zirconium exhibited a strong correlation ( $r_s \geq 0.94$ ,  $p < 0.01$ ) in the whole studied area, which can be explained by the presence of zircon [ZrSiO<sub>4</sub>], up to 4%, in the composition of the predominant gneiss rocks in the region (Machado, 2008). Since Hf appears naturally bound to the minerals Zr, both elements are found in a fixed proportion (Rudnick & Gao, 2014), which was verified by fitting the concentrations detected in the samples to a linear function (see Fig. S3). Additionally, in the three mining areas Hf and Zr showed strong positive correlations with Ta ( $r_s \geq 0.84$ ,  $p < 0.01$ ), and all three exhibited positive correlations ( $0.59 \leq r_s \leq 0.97$ ,  $p < 0.01$ ) with Al, Ba, and Rb and negative correlations with Cs ( $r_s \sim -0.77$ ,  $p < 0.01$ ). The correlations observed suggest that the presence of Hf, Ta, and Zr in the soils may be of lithogenic origin.

The contents of Th and U were significantly correlated in the three mining areas (IMA:  $r_s = 0.92$ , UMA:  $r_s = 0.95$ , and VMA:  $r_s = 0.83$  at  $p < 0.01$ ). Uranium deposits in Caetité originated from an albitization process followed by a subsequent hydrothermal event (Pascholati et al., 2003). For that reason, they are associated with rock dominated by plagioclase (albite + oligoclase) and albitites, as well as other minerals such as andradite [Ca<sub>3</sub>Fe<sub>2</sub>(SiO<sub>4</sub>)<sub>3</sub>],

calcite [CaCO<sub>3</sub>], thorite [(Th,U)SiO<sub>4</sub>], and thorianite [ThO<sub>2</sub>], which are very abundant in the region (Lobato et al., 2015). At the same time, these minerals are associated with biotite, feldspar, and zircon, which would explain the positive correlations ( $0.54 \leq r_s \leq 0.88$ ) between these two elements and Al, Ba, Fe, K, Hf, Ta, and Zr.

It was observed that all REE, except Sc, form a highly correlated group ( $r_s \geq 0.88$ ,  $p < 0.01$ ). They also showed important correlations within the range  $0.55 \leq r_s \leq 0.86$  with Al, Ba, Hf, K, Rb, Ta, Th, U, and Zr. These findings are mainly associated with the mineralogical composition of the region. Due to some similar chemical characteristics that these elements share, the REE can substitute themselves in various crystal lattices. This ability leads to multiple REE occurrences within a single mineral, such as allanite [(Ca,Ce,La)<sub>2</sub>(Al,Fe)<sub>3</sub>(SiO<sub>4</sub>)<sub>3</sub>OH], bastnaesite [(Ce,La,Nd)CO<sub>3</sub>F], monazite [(Ce,La)PO<sub>4</sub>], and xenotime [(Dy,Yb)PO<sub>4</sub>] (Wang & Liang, 2015). Although monazite is the mineral type with the highest occurrence in Brazil (De Sá Paye et al., 2016), the study area also presents occurrences of allanites (up to 2%) and xenotimes (up to 1%). These minerals are associated with biotite, feldspars, thorianite, and zircon (Machado, 2008), which explains the correlation observed with the other elements.

On the contrary, Sc did not present significant correlations with the other REE. In this case, the highest positive correlations for Sc were with Cs ( $r_s \sim 0.74$ ,  $p < 0.01$ ) and Fe ( $r_s$ : 0.83,  $p < 0.01$ ) in the three areas, as well as with Ti ( $r_s \sim 0.70$ ,  $p < 0.01$ ) in UMA and VMA. These findings suggest that Sc and REE do not share a similar origin. Likewise, Ti did not show significant correlations with the other HFSE. Its main correlations throughout the region were with Fe, especially in IMA ( $r_s = 0.87$ ,  $p < 0.01$ ), which may be associated with the iron deposits.

According to the values of Spearman correlation coefficients, it was observed that PTE can be divided into two main groups. The first includes As, Co, Cr, Cu, Mn, Ni, and V, which showed strong positive correlations ( $r_s \geq 0.71$ ,  $p > 0.01$ ) between them. These elements also exhibited strong positive correlations with Cs, Fe, Sc, and Ti. Specifically, in IMA and VMA, some correlations observed such as Cr–Fe–Mn and Ni–Ti–V can be associated with the presence of chromite [FeCr<sub>2</sub>O<sub>4</sub>] and vanadium–titanium

magnetite minerals. In contrast, this group of elements showed negative correlations ( $r_s \geq -0.61$ ) with Ba, Hf, Rb, and Zr, thus suggesting opposite sources of origin in the three mining areas.

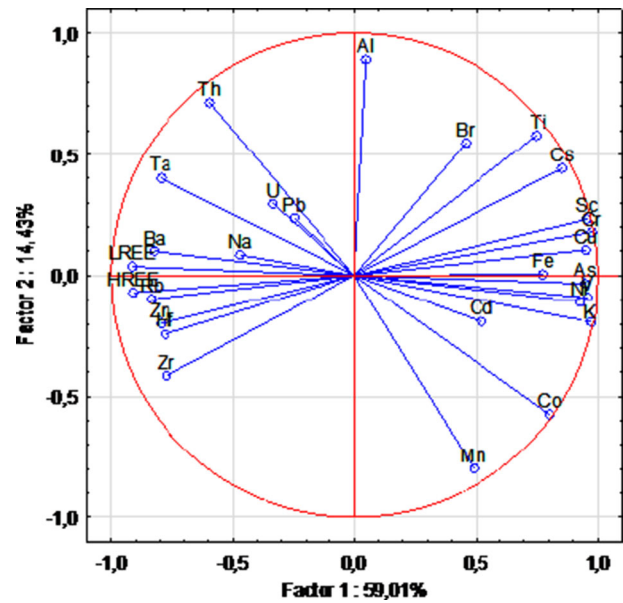
The second group comprises Br, Cd, Pb, and Zn that individually presented fewer relationships with the other PTE. Bromine shows positive correlations ( $0.60 \leq r_s \leq 0.67$ ) with Al and Pb, as well as negative correlations with Hf and Rb. In UMA, Cd exhibited moderate positive correlations with As ( $r_s = 0.60$ ) and K ( $r_s = 0.66$ ) for  $p < 0.01$ , and a strong correlations with Fe ( $r_s = 0.86$ ). In IMA, the highest correlations between As–Cd–Fe were observed ( $r_s \geq 0.82$ ), suggesting that in this area the presence of these elements in soils may be related to iron mining activities. Since Cd was not quantified in VMA, no correlations were observed. In the case of Pb, it was mainly correlated ( $0.53 \leq r_s \leq 0.90$ ) with elements of natural origin such as REE, Th, and U, especially in the Caetité region (IMA and UMA). Finally, Zn was mainly correlated with Al, Ba, Rb, and REE.

In this work, the PCA was performed for all the available elements in order to provide the most comprehensive explanatory perspective. Since PCA results can be affected by dimensionality, the sums of LREE (except Sc) and HREE were performed to reduce the number of variables and improve the issue of dimensionality. The PCA of the analyzed elements in soils from the UMA region is shown in Fig. 7. Analogous graphs showing the PCA results for the IMA and VMA regions are presented in Figures S4a–b (Supplementary Material). Table S11 summarizes the total variance (%), the eigenvalues of each principal component, as well as the variable loadings of PC1 and PC2 for the three mining areas.

The application of the PCA method for the analysis of metals in soils from the UMA region grouped the elements into two main components that explain 73.4% of the variance. PC1 is the most important component, since it accounts for the highest total variance (59.01%) and divided the elements into two main groups. Based on the correlation analysis and the geological characteristics of the region, the elements grouped on the left (negative loadings) may come from geogenic sources, while the elements on the right side (positive loadings) are likely associated with diverse anthropogenic sources.

The second component (PC2) explained 14.42% of the total variance, and the strongest loadings were

**Fig. 7** PCA results for the elements determined in soils from the UMA region



observed for Al (0.89) and Mn (−0.80). PC2 is supposed to provide information on sources of pollution that introduce and/or redistribute metals in soils. Elements at the top (positive loadings) can be associated with industry, mining, and other sources of pollution typical of urban areas, such as ceramic industry and traffic emissions, while the elements at the bottom (negative charges) can have their main source in agriculture. It is well known that Al, Fe, Sc, Ti, and PTE are commonly found in wastes from industrial and mining activities (Akinci & Guven, 2019). Likewise, particles from the vehicle exhaust gases can be the main cause of the high concentrations of Br in soils, as this element has traditionally been used as an additive in gasoline. On the other hand, the application of phosphate fertilizers, pesticides, and fungicides to maximize agricultural yield dramatically increases the contents of As, Cd, Co, K, and Mn (among other PTE) (Shi et al., 2018).

For the IMA and VMA regions, the PCA results showed the same general behaviors with slight differences (Figs. S4a-b). PC1 explained the highest percentage of the total variance in both regions (IMA:48.2% and VMA: 42.1%). It also separated the elements into groups quite similar to those shown for the UMA region (Fig. 7). The main difference in IMA is that K, Mn, and Ti exhibited significant negative loadings ( $\geq -0.93$ ), indicating that these elements have a natural origin, mainly related to the presence of

iron minerals, as mentioned above. Similarly, K is located in the category of elements of geogenic origin in the VMA region (loading: −0.67), a fact that can be linked to the predominance of alkaline feldspars that exists in that region (De Queiroz, 2016).

In IMA, elements with positive charges for PC2 (As, Br, Cd, Fe, and Sc) can be directly associated with iron extraction operations, since the highest concentrations of As and Cd were detected in soil samples collected near the mine. Furthermore, these elements exhibited strong positive correlations with Fe in this region. Although elements with negative loadings (Co, Cr, Cs, Cu, Ni, and V) are also related to mining activity, the fact that they are in another group suggests that the main contributions come from other sources such as auto repair shops (common in the districts visited), domestic wastes, and the weathering of building surfaces and pavements, which contribute to the presence of these pollutants in the nearby soils (Doabi et al., 2018; Wu et al., 2018). In the case of the VMA region, all items are included in the same category with respect to the PC2 classification. This indicates that mining can be considered as the main source of contamination in that region. However, given that in the Maracás region all the samples were collected in the rural area, the contribution of agriculture should not be disregarded.

The weak loadings ( $< 0.35$ ) observed for Pb and U in Caetité region (IMA and UMA), as well as, for Al

and Zn in Maracás indicate that even though these elements have a predominantly geogenic origin, their current content in soils may have been altered by both natural processes (erosion and atmospheric deposition) and by anthropogenic sources (mining, agriculture and industry). The case of Pb is interesting because this is an element derived mainly from industrial activities. However, in the Caetité region its presence in soils seems to be associated with Th and U, since the radioactive series of both elements end in stable isotopes of Pb.

The dendrogram of the elements analyzed in the soils of the total study area reveals two main clusters (Fig. 8a). The first cluster includes the elements considered of natural origin, which matches PCA results, and reinforces the geogenic origin of these elements. Smaller groups such as Ba-Rb, LREE-HREE-Zn, Hf-Zr, and Ta-Th reinforce the previously discussed correlations. As can be seen, Al and U are weakly associated with this cluster, suggesting that they have been somewhat altered by human activities. The second cluster is made up of elements related to anthropogenic sources. Likewise, the As-Cd-Fe and Cr-Cs-Cu-Ti-V-Sc-Ni groups confirmed some of the aforementioned interrelationships. Lead appears weakly associated with cluster 2, reflecting the mixed geogenic-anthropogenic origin of this metal. Therefore, it can be considered as a pseudo-natural element.

The HCA also identified two main groups of association between sampling locations in the study area (Fig. 8b). The cluster on the right side includes only sites from the Caetité region (IMA and UMA) and is made up of three subgroups. The first one (SL-07 to SL-15) contains soils from the cities of Caetité, Lagoa Real, and the Maniaçu district. The second (SL-02 to SL-12) and the third (SL-19 to SL-21) group natural and agricultural soils collected near the uranium and iron mines, respectively. The cluster on left side combines natural and agricultural soils from both municipalities (SL-06 to SL-25) with urban soils collected in Maracás (SL-24 to SL-31). The sites in the vicinity of the vanadium mine (SL-27 to SL-29) form the last subgroup of this cluster.

#### Comparison with similar studies worldwide

The average concentrations of some elements analyzed in this study were compared with similar studies from other countries, in which mining is an important

economic activity (Table 2). This table also shows the concentration values of metals reported for important urban areas around the world and agricultural soils. The highest concentration value for each metal was underlined.

The average values of Al, Ba, Co, Fe, and V reported in this study are higher than those of the other mining areas. Besides, the values of Mn, Th, and U are the second highest, thus indicating that more than 50% of the elements listed in Table 2 have significant concentrations in the study area. In the case of urban soils, only Al, Ba, and Ni presented a higher average compared to that reported for the other urban areas, and Cr showed the second-highest concentration just below the Chinese city of Xiangyang. Concerning the agricultural soils, the concentration of Cd and Fe are the highest, and Co, Cr, and Mn values are among the highest reported for this type of soils. It can be seen that concentrations of elements are very heterogeneous, which is the result of the different geological and climatic characteristics, as well as the agricultural methods and techniques used in each country.

#### Conclusions

This work presents a detailed study of soil contamination in three mining areas of the semiarid region of Bahia (NE-Brazil). From the statistical analyzes carried out, the group of elements formed by: Al, Ba, Hf, K, Na, Pb, Rb, REE, Ta, Th, U, Zn, and Zr could be considered mainly of geogenic origin, since they are related to the lithological background of the region, *i.e.*, granitic-gneissic rocks with important mineral occurrences (albite, feldspar, allanite, biotite, monazite, torianite, zircon, etc.). On the other hand, As, Br, Cd, Co, Cr, Cs, Cu, Fe, Mn, Ni, Sc, Ti, and V are predominantly of anthropogenic origin.

The calculated pollution indices revealed that the region can be classified as severely contaminated, since the soils from the mining areas presented a moderate to high level of contamination for 89% of the elements analyzed. Additionally, an extreme level of contamination (for at least one element) was observed in 78% of the sampling points, thus confirming the impacts of multiple anthropogenic activities on soil quality. On a regional scale, mining and agriculture are the main sources of pollution, followed by industrial, domestic, and traffic emissions. These activities are

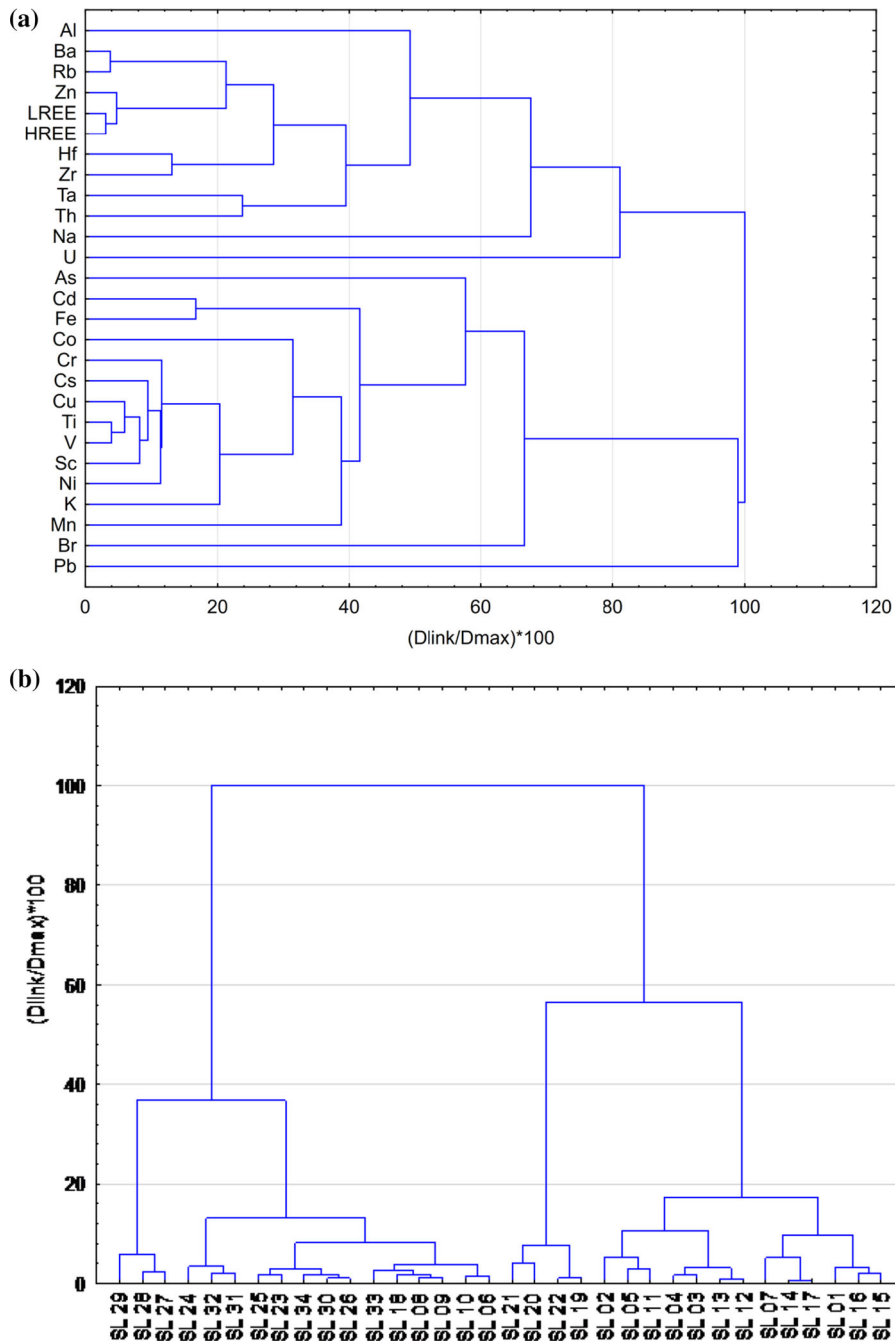


**Fig. 8** Dendrograms obtained by hierarchical clusters analysis for: **a** the elements determined in soils of the total region. **b** all sampling locations in the study area

responsible not only for introducing pollutants such as PTE into the soil but also for modifying and redistributing the content of natural elements such as Al, K, Pb, and U.

It should be noted that most of the soils from the study region exhibited contents of Al, As, Ba, Cd, Cr, Fe, Ni, REE, and U above the limits recommended by Brazilian and/or US laws. Taking into account that these are inhabited areas, exposure to these pollutants

**Table 2** Comparison of the average concentration of 15 elements of interest reported in this study with those of similar studies worldwide (values in mg kg<sup>-1</sup> unless % indicated)

	Al %	As	Ba	Cd	Co	Cr	Cu	Fe %	Mn	Ni	Pb	Th	U	V	Zn
<b>Soils from mining areas</b>															
China ( <i>n</i> = 73) <sup>a</sup>	–	196	–	11.0	6.82 <sub>b</sub>	84.3	211.9	–	386.5 <sub>b</sub>	106.6	<u>641.3</u>	<u>51.5<sub>b</sub></u>	<u>34.7<sub>b</sub></u>	–	<u>1163</u>
Ghana ( <i>n</i> = 4) <sup>c</sup>	3.3	102	–	0.1	8.78	64.6	27.2	2.2	366.2	16.3	10.8	–	–	55.3	36.6
India ( <i>n</i> = 5) <sup>a</sup>	–	19	–	3.8	–	<u>1509</u>	63.5	–	–	1069	304.7	–	–	–	338.8
Iran ( <i>n</i> = 3) <sup>a</sup>	–	146	–	1.5	–	–	88.4	–	–	–	1002	–	–	–	363.4
South Korea ( <i>n</i> = 70) <sup>a</sup>	–	70	–	2.0	–	–	79.1	–	–	22.0	111.1	–	–	–	183.2
Turkey ( <i>n</i> = 1) <sup>d</sup>	3.3	940	–	–	–	46.6	14.8	2.2	314.2	52.0	–	–	–	–	124.4
United State ( <i>n</i> = 4) <sup>e</sup>	4.1	10	428	0.2	8.1	33.0	20.0	1.9	<u>565.0</u>	17.0	15.4	7.7	2.1	43.0	49.0
Vietnam ( <i>n</i> = 3) <sup>a</sup>	–	<u>3144</u>	–	<u>135</u>	–	1501	<u>271.4</u>	–	–	<u>2254</u>	30.6	–	–	–	41.1
This study ( <i>n</i> = 3)	<u>8.8</u>	5.0	<u>812</u>	4.1	<u>11.1</u>	51.9	8.2	<u>9.8</u>	502.1	24.7	9.2	22.0	5.1	<u>98.5</u>	70.2
<b>Urban Soils</b>															
Chile (Taltal city) <sup>f</sup>	1.6	<u>37.9</u>	125	0.6	<u>20.6</u>	19.3	<u>766.8</u>	<u>5.5</u>	<u>865.4</u>	21.1	135.3	–	–	<u>120.9</u>	224.1
China (Xiangyang) <sup>g</sup>	–	28.4	–	3.7	–	<u>3156</u>	69.2	–	–	45.3	76.7	–	–	–	116.9
Italy (Naples) <sup>f</sup>	–	12.4	–	0.5	–	12.5	163	–	–	–	100	–	–	–	142.0
Nigeria (Ibadan) <sup>f</sup>	–	3.9	–	<u>8.4</u>	–	64.4	46.8	–	–	–	95.1	–	–	–	<u>228.6</u>
Scotland (Glasgow) <sup>f</sup>	–	9.0	–	–	–	52.0	52.0	–	–	–	<u>195</u>	–	–	–	178.0
This study	<u>10.3</u>	4.5	<u>777</u>	1.8	10.6	75.8	12.5	4.6	574.5	<u>83.7</u>	10.4	32.8	9.0	93.0	59.4
<b>Agricultural Soils</b>															
Colombia <sup>h</sup>	–	–	–	0.04	–	–	<u>1149</u>	–	–	<u>661</u>	0.07	–	–	–	<u>1365</u>
Iran <sup>j</sup>	–	–	–	–	–	<u>79.2</u>	41.2	–	5.73 <sup>j</sup>	131.4	–	–	–	–	74.6
Pakistan <sup>k</sup>	–	–	–	1.08	<u>15.0</u>	22.2	15.8	0.5	331.6	13.4	<u>54.6</u>	–	–	–	74.0
Turkey <sup>l</sup>	–	–	–	1.48	9.1	43.8	22.5	–	<u>629.8</u>	61.1	19.7	–	–	–	41.2
This study	10.8	2.8	789	<u>2.12</u>	10.1	45.2	10.1	<u>4.6</u>	590.6	48.0	8.9	30.9	7.2	64.0	87.5

*n* = number of examined mines; “–”: values not reported

<sup>a</sup> Li et al., 2014;

<sup>b</sup> Wang et al., 2019;

<sup>c</sup> Hadzi et al., 2019;

<sup>d</sup> Akinci & Guven, 2019;

<sup>e</sup> Bern et al., 2019;

<sup>f</sup> Reyes et al., 2019;

<sup>g</sup> Wu et al., 2018;

<sup>h</sup> Marrugo-Negrete et al., 2017; <sup>i</sup> Doabi et al., 2018;

<sup>j</sup> Keshavarzi and Kumar et al., 2019;

<sup>k</sup> Shah et al., 2019;

<sup>l</sup> Sungur et al., 2015

by direct contact or accidental ingestion can pose a risk to human health (lung and kidney cancer, skin lesions, brain damage, cardiovascular and

cerebrovascular diseases, etc.). That is why, the authors want this study to draw the attention of competent organisms concerning the need for new

laws and strategies for preservation of the soils especially in vulnerable zones such as mining areas. For example, green and affordable technologies such as phytoremediation, which have been used successfully to extract or remove PTE (As, Cd, Hg, and Pb) from contaminated soils, would be an effective solution to improve environmental quality in these semiarid regions. Finally, we hope that the methods adopted and the data reported in this work could be useful for the international scientific community to evaluate, control, and discuss the impacts of mining on environment.

**Acknowledgements** This study was funded in part by the Coordination of Improvement of Higher Education Personnel – Brazil (CAPES) and by the State University of Santa Cruz (UESC), Bahia—Brazil. The authors would like to thank the staff of the Research Reactor Center (CRPq) belonging to the Nuclear and Energy Research Institute (IPEN), for the technological support and the Research Laboratory in Analytical Chemistry (LPQA) of the UESC for the logistic support provided for the ICP OES analysis. We appreciate the contribution (maps elaboration) of Romario Oliveira de Santana, a Ph.D. PRODEMA-UESC student. Finally, we would like to thank all the colleagues of the Center for Research in Radiation Sciences and Technologies (CPqCTR) for their support in carrying out this work.

**Author's contribution** Diango M. Montalván Olivares was involved in substantial contributions to conception and design of the study, acquisition of data, analysis and interpretation of data, drafting the article and critical review. Caroline Santana contributed to acquisition and analysis of data, drafting the article. Fermin Garcia Velasco helped in contributions to conception of the study, critical review of important intellectual content, final approval of the version to be submitted for publication. Francisco H. Martinez Luzardo was involved in contributions to conception of the study, drafting the article and critical review of important intellectual content. Sergio Fred Ribeiro Andrade helped in acquisition of data. Regina Beck Ticianelli contributed to analysis and interpretation of data. Maria Jose Armelin helped in analysis and interpretation of data. Frederico Genezini was involved in critical review of important intellectual content, final approval of the version to be submitted for publication. All authors agreed to publish the manuscript respecting the current sequence of authors listed. Likewise, all authors agreed to designate Diango M. Montalván as the corresponding author of the submission.

**Funding** The research funders were already mentioned in the acknowledgments. All authors certify that they have no financial interest in the subject or the materials discussed in this manuscript.

## Declarations

**Human or animal rights** Since this study did not involve human and animal research, no consents were required to participate and/or publish biological material or data belonging to humans and/or animals. Therefore, the inclusion of these forms and other ethical issues related to the publication of this type of data do not apply to this study

**Consent for publish** AAll authors agree to publish the manuscript respecting the current sequence of authors listed. Likewise, all authors agreed to designate Diango M. Montalván as the corresponding author of the submission.

## References

- Akinci, G., & Guven, D. E. (2019). Assessment of chemical fractionations and mobilization potentials for heavy metals in wastes and other solid matrices in a mining site in the inland Aegean Region in Turkey. *Environmental Monitoring and Assessment*, *191*, 25–38. <https://doi.org/10.1007/s10661-018-7158-5>
- Bahia Mineração (BAMIN). *Pedra de Ferro Project* [online]. Salvador: BAMIN, 2016 [viewed: March, 11th, 2020]. Available: <https://www.bamin.com.br/ing/pagina.php?cod=1>
- Bern, C. R., Walton-Day, K., & Naftz, D. L. (2019). Improved enrichment factor calculations through principal component analysis: Example from soils near breccia pipe uranium mines, Arizona, USA. *Environmental pollution*, *248*, 90–100. <https://doi.org/10.1016/j.envpol.2019.01.122>
- Biondi, C. M., Nascimento, C. W. A., Neta, A. B. F., & Ribeiro, M. R. (2011). Teores de Fe, Mn, Zn, Cu, Ni e Co em solos de referência de Pernambuco. *Revista Brasileira de Ciência do Solo*, *35*, 1057–1066
- Bonotto, D. M. (2015). <sup>226</sup>Ra and <sup>228</sup>Ra in mineral waters of southeast Brazil. *Environmental Earth Sciences*, *74*, 839–853. <https://doi.org/10.1007/s12665-015-4088-1>
- Burritt, R. L., & Christ, K. L. (2018). Water risk in mining: Analysis of the Samarco dam failure. *Journal of Cleaner Production*, *178*, 196–205. <https://doi.org/10.1016/j.jclepro.2018.01.042>
- Centro de Tecnologia Mineral (CETEM). **Exploração de minério de ferro em Caetité (BA) afeta meio ambiente e comunidades locais**. Ministério de Ciência e Tecnologia, Rio de Janeiro, 2013.
- Chauvel, C., & Rudnick, R. L. (2016). **Large-ion Lithophile Elements** In W. White (Eds.), *Encyclopedia of Geochemistry. Encyclopedia of Earth Sciences Series*. Springer, Cham. [https://doi.org/10.1007/978-3-319-39193-9\\_232-1](https://doi.org/10.1007/978-3-319-39193-9_232-1).
- Conselho Nacional do Meio Ambiente (CONAMA). **Resolução N° 420**, December 28<sup>th</sup>, 2009. Ministry of Environment, Brazil. DOU n° 249, 2009.
- Da Silva, Y. J. A. B., Do Nascimento, C. W. A., Cantalice, J. R. B., Da Silva, Y. J. A. B., & Cruz, C. M. C. A. (2015). Watershed-scale assessment of the background

- concentrations and guidance values for heavy metals in soils from a semi-arid and coastal zone of Brazil. *Environmental Monitoring and Assessment*, 187, 558–568. <https://doi.org/10.1007/s10661-015-4782-1>
- De Geer, L. E. (2004). Currie detection limits in gamma-ray spectroscopy. *Applied Radiation Isotopes*, 61, 151–160. <https://doi.org/10.1016/j.apradiso.2004.03.037>
- De Paula, F. C. F., & Abrahão, J. R. S. (1991). Geochemical prospecting for vanadium and chromium in the Iramaia sheet, Bahia State, Brazil. *Journal of Geochemical Exploration*, 41, 125–135.
- De Queiroz, T. D. A., 2016. Geological mapping, petrography, litho-geochemical and geophysical aspects of the Maracás region (FOLHA SD.24-V-D-I), Dissertation presented to the Geosciences Institute of the Federal University of Bahia, Bahia, Brazil.
- De Sá Paye, H., De Mello, J. W., De Magalhães Mascarenhas, G. R. L., & Gasparon, M. (2016). Distribution and fractionation of the rare earth elements in Brazilian soils. *Journal of Geochemical Exploration*, 161, 27–41. <https://doi.org/10.1016/j.gexplo.2015.09.003>
- Do Carmo, F. F., Kamino, L. H. Y., Junior, R. T., De Campos, I. C., Do Carmo, F. F., Silvino, G., De Castro, K. J. S. X., Mauro, M. L., Rodrigues, N. U. A., Miranda, M. P. S., & Pinto, C. E. F. (2017). Fundão tailings dam failures: the environment tragedy of the largest technological disaster of Brazilian mining in global context. *Perspectives in ecology and conservation*, 15, 145–151. <https://doi.org/10.1016/j.pecon.2017.06.002>
- Doabi, S. A., Karami, M., Afyuni, M., & Yeganeh, M. (2018). Pollution and health risk assessment of heavy metals in agricultural soil, atmospheric dust and major food crops in Kermanshah province, Iran. *Ecotoxicology and Environmental Safety*, 163, 153–164. <https://doi.org/10.1016/j.ecoenv.2018.07.057>
- Doležalová, H. W., Mihočová, S., Chovanec, P., & Pavlovský, J. (2019). Potential ecological risk and human health risk assessment of heavy metal pollution in industrial affected soils by coal mining and metallurgy in Ostrava, Czech Republic. *International journal of environmental research and public health*, 16, 4495
- Brazilian Agricultural Research Corporation (EMBRAPA). **Documento 115: Amostragem e cuidados na coleta de solo para fins de fertilidade**. Manaus, AM: EMBRAPA, 2014.
- Eurasian Natural Resources Corporation (ENRC). **Deposit geology and the Fe ore project in Caetité, Bahia**. 2012. [www.enrc.com](http://www.enrc.com)
- Fernandes, H. M., Gomiero, L. A., Peres, V., Franklin, M. R., & Simões Filho, F. F. L. (2008). Critical analysis of the waste management performance of two uranium production units in Brazil—part II: Caetite production center. *Journal of Environmental Management*, 88, 914–925. <https://doi.org/10.1016/j.jenvman.2007.04.022>
- Fernandes, H. M.; Franklin, M. R.; Leoni, G. M.; Almeida, M. (2004). **A case study on the Uranium tailings dam of Poços de Caldas uranium mining and milling site**. IAEA-TECDOC—1403.
- Fordyce, F. M., Everett, P. A., Bearcock, J. M., & Lister, T. R. (2019). Soil metal/metalloid concentrations in the Clyde Basin, Scotland, UK: Implications for land quality. *Earth and Environmental Science Transactions of the Royal Society of Edinburgh*, 108, 191–216. <https://doi.org/10.1017/S1755691018000282>
- Fosu-Mensah, B. Y., Ofori, A., Ofosuhen, M., Ofori-Attah, E., Nunoo, F. E., Darko, G., Tuffor, I., Gordon, C., Arhinful, D. K., Nyarko, A. K., & Appiah-Opong, R. (2018). Assessment of heavy metal contamination and distribution in surface soils and plants along the West Coast of Ghana. *West African Journal of Applied Ecology*, 26, 167–178
- Hadzi, G. Y., Ayoko, G. A., Essumang, D. K., & Osae, S. K. D. (2019). Contamination impact and human health risk assessment of heavy metals in surface soils from selected major mining areas in Ghana. *Environmental Geochemical Health*, 41, 2821–2843. <https://doi.org/10.1007/s10653-019-00332-4>
- Indústrias Nucleares do Brasil (INB). *INB Caetité - Unidade de Concentrado de Urânio* [online]. Rio de Janeiro: Indústrias Nucleares do Brasil, 2020 [viewed: March 09th, 2020]. Available from: <http://www.inb.gov.br/pt-br/A-INB/Onde-estamos/Caetite/C3%A9>.
- Instituto Brasileiro de Mineração (IBRAM). **Relatório Anual das Atividades Janeiro 2019- Dezembro de 2019**. Brasília: IBRAM, 2020.
- Instituto de Pesquisas Energéticas e Nucleares (IPEN). *Reator de pesquisas IEA-RI* [online]. São Paulo: Instituto de Pesquisas Energéticas e Nucleares, 2020 [viewed: March, 16th, 2020]. Available from: [https://www.ipen.br/portal\\_por/portal/interna.php?secao\\_id=729](https://www.ipen.br/portal_por/portal/interna.php?secao_id=729).
- International Atomic Energy Agency (IAEA). **Update of X Ray and Gamma Ray Decay Data Standards for Detector Calibration and Other Applications**. Volume 1: Recommended Decay Data, High Energy Gamma Ray Standards and Angular Correlation Coefficients. Vienna: IAEA, 2007.
- International Atomic Energy Agency (IAEA). **Environmental Contamination from Uranium Production Facilities and their Remediation**. Vienna: IAEA, 2005.
- International Organization For Standardization (ISO). Soil Quality. Extraction of Trace Elements Soluble in Aqua Regia. ISO 11466, 1995.
- International Union of Pure and Applied Chemistry (IUPAC). (1978). Analytical chemistry division. Commission on spectrochemical and optical procedure for analysis. Nomenclature, symbols, units and their usage in spectrochemical analysis—II. data interpretation Analytical chemistry division. *Spectrochimica Acta Part B: Atomic Spectroscopy*, 33(6), 241–245.
- Järup, L. (2003). Hazard of heavy metal contamination. *British Medical Bulletin*, 68, 167–182. <https://doi.org/10.1093/bmb/ldg032>
- Jiang, S. Y., Wang, R. C., Xu, X. S., & Zhao, K. D. (2005). Mobility of high field strength elements (HFSE) in magmatic-, metamorphic-, and submarine-hydrothermal systems. *Physics and Chemistry of the Earth, Parts A/B/C*, 30, 1020–1029. <https://doi.org/10.1016/j.pce.2004.11.004>
- Jinxia, L., Mei, H., Xiuqin, Y., & Jiliang, L. (2010). Effects on the accumulation of the rare earth elements on soil macrofauna community. *Journal of Rare Earths*, 28, 957–965. [https://doi.org/10.1016/S1002-0721\(09\)60233-7](https://doi.org/10.1016/S1002-0721(09)60233-7)
- Keshavarzi, A., & Kumar, V. (2019). Ecological risk assessment and source apportionment of heavy metal contamination in

- agricultural soils of Northeastern Iran. *International Journal of Environmental Health Research*, 29, 544–560. <https://doi.org/10.1080/09603123.2018.1555638>
- Kumar, A., Narang, S., Mehra, R., & Singh, S. (2017). Assessment of radon concentration and heavy metal contamination in groundwater samples from some areas of Fazilka district, Punjab, India. *Indoor and Built Environment*, 26, 368–374. <https://doi.org/10.1177/1420326X15591639>
- Largo Resources Ltd. *Maracás Menchen Mine* [online]. Toronto: Largo Resources, 2020 [viewed: March, 11th, 2020]. Available: <https://www.largoresources.com/operations/maracas-menchen-mine/default.aspx>
- Li, Z., Ma, Z., van der Kuijp, T. J., Yuan, Z., & Huang, L. (2014). A review of soil heavy metal pollution from mines in China: Pollution and health risk assessment. *Science of the Total Environment*, 468–469, 843–853. <https://doi.org/10.1016/j.scitotenv.2013.08.090>
- Ling, Q., Dong, F., Yang, G., Han, Y., Nie, X., Zhang, W., & Zong, M. (2019). Spatial distribution and environmental risk assessment of heavy metal identified in soil of a decommissioned uranium mining area. *Human and Ecological Risk Assessment: An International Journal*. <https://doi.org/10.1080/10807039.2019.1630601>
- Lobato, L. M., Pimentel, M. M., Cruz, S. C., Machado, N., Noce, C. M., & Alkmim, F. F. (2015). U-Pb geochronology of the Lagoa real uranium district, Brazil: Implications for the age of the uranium mineralization. *Journal of South American Earth Sciences*, 58, 129–140. <https://doi.org/10.1016/j.jsames.2014.12.005>
- Lyu, S., Wei, X., Chen, J., Wang, C., Wang, X., & Pan, D. (2017). Titanium as a beneficial element for crop production. *Frontiers in Plant Sciences*, 8, 597. <https://doi.org/10.3389/fpls.2017.00597>
- Machado, G. D. S. (2008). *Geologia da porção sul do complexo Lagoa Real*. Caetité-BA. Instituto de Geociências da Universidade Federal da Bahia.
- Marrugo-Negrete, J., Pinedo-Hernández, J., & Díez, S. (2017). Assessment of heavy metal pollution, spatial distribution and origin in agricultural soils along the Sinú River Basin, Colombia. *Environmental Research*, 154, 380–388. <https://doi.org/10.1016/j.envres.2017.01.021>
- Mughabghab, S. F. (2003). **Thermal neutron capture cross sections resonance integrals and g-factors**. International Nuclear Data Committee-IAEA.
- Pascholati, E. M., Da Silva, C. L., Costa, S. D. S., Osako, L. S., Amaral, G., & Rodriguez, I. P. (2003). Novas ocorrências de urânio na região de lagoa real, a partir da superposição de dados geofísicos, geológicos e de sensoriamento remoto. *Revista Brasileira de Geociências*, 33, 91–98
- Planejamento Ambiental e Arquitetura Ltda (PLANARQ). **Estudo de Impactos Ambientais: Unidade de Concentrado de Urânio em Caetité**. Indústrias Nucleares do Brasil (INB). Salvador, Bahia: 1997.
- Railsback, L. B. (2003). An earth scientist's periodic table of the elements and their ions. *Geology*, 31, 737–740. <https://doi.org/10.1130/G19542.1>
- Reyes, A., Thiombane, M., Panico, A., Daniele, L., Lima, A., Di Bonito, M., & De Vivo, B. (2019). Source patterns of potentially toxic elements (PTEs) and mining activity contamination level in soils of Taltal city (northern Chile). *Environmental Geochemistry Health*. <https://doi.org/10.1007/s10653-019-00404-5>
- Rudnick RL, Gao S (2014) Composition of the continental crust. In: Treatise on geochemistry. Holland H, Turekian K, (pp. 1–51), Elsevier, Berlin
- Shah, M. H., Ilyas, A., Akhter, G., & Bashir, A. (2019). Pollution assessment and source apportionment of selected metals in rural (Bagh) and urban (Islamabad) farmlands, Pakistan. *Environmental Earth Sciences*, 78, 189. <https://doi.org/10.1007/s12665-019-8198-z>
- Shi, T., Ma, J., Wu, X., Ju, T., Lin, X., Zhang, Y., Li, X., Gong, Y., Hou, H., Zhao, L., & Wu, F. (2018). Inventories of heavy metal inputs and outputs to and from agricultural soils: A review. *Ecotoxicology and Environmental Safety*, 164, 118–124. <https://doi.org/10.1016/j.ecoenv.2018.08.016>
- Sungur, A., Soylak, M., Yilmaz, E., Yilmaz, S., & Ozcan, H. (2015). Characterization of heavy metal fractions in agricultural soils by sequential extraction procedure: The relationship between soil properties and heavy metal fractions. *Soils and Sediment Contamination: An International Journal*, 24, 1–15. <https://doi.org/10.1080/15320383.2014.907238>
- Tchounwou, P.B.; Yedjou C.G.; Patlolla, A.K.; Sutton, D.J. **Heavy metal toxicity and the environment**. in: LUCH, A. (Ed.). **Molecular, Clinical and Environmental Toxicology**. 1<sup>st</sup> ed. Basel: Springer, 2012. Vol. 3, cap. 6, p. 133–164. DOI: [https://doi.org/10.1007/978-3-7643-8340-4\\_6](https://doi.org/10.1007/978-3-7643-8340-4_6).
- Tomlinson, D. C., Wilson, J. G., Harris, C. R., & Jeffrey, D. W. (1980). Problems in the assessment of heavy metals levels in estuaries and the formation of a pollution index. *Helgolander Meeresunters*, 33, 566–575. <https://doi.org/10.1007/BF02414780>
- United States Environmental Protection Agency (USEPA). **Soil sampling quality assurance user's guide – EPA 600/8–89/046**. 2<sup>nd</sup> ed. Washington-DC: USEPA, 1989a.
- United States Environmental Protection Agency (USEPA). *Regional Screening Level Summary Table* [online]. Washington D.C.: United States Environmental Protection Agency, 2019 [viewed: March 24th, 2020]. Available from: <https://www.epa.gov/risk/regional-screening-levels-rsls-generic-tables>
- Van Zyl Dirk, J.A.; Straskraba, V. (1999). **Mine closure considerations in arid and semi-arid areas**. Mine, water and environment. IMWA Congress.
- Wang, L., & Liang, T. (2015). Geochemical fractions of rare earth elements in soil around a mine tailing in Baotou China. *Scientific Reports*, 5, 12483. <https://doi.org/10.1038/srep12483>
- Wang, Z., Qin, H., & Liu, X. (2019). Health risk assessment of heavy metals in the soil-water-rice system around the Xiaozhuang uranium mine China. *Environmental Science and Pollution Research*, 26, 5904–5912. <https://doi.org/10.1007/s11356-018-3955-1>
- World Information Service on Energy (WISE) – URANIUM PROJECT. *Chronology of major tailings dam failure* [online]. Arnsdorf, Germany: Peter Diehl, 2019 [viewed: March 6th, 2020]. Available from: <http://www.wise-uranium.org/mdaf.html>
- Wu, W., Wu, P., Yang, F., Sun, D., Zhang, D., & Zhou, Y. (2018). Assessment of heavy metal pollution and human

health risk in urban soils around an electronics manufacturing facility. *Science of the Total Environment*, 630, 53–61. <https://doi.org/10.1016/j.scitotenv.2018.02.183>

Zahn, G. S., Junqueira, L. S., & Genezini, F. A. (2019). CAX and Xsel: A software bundle to aid in automating NAA spectrum analysis. *Brazilian Journal of Radiation Sciences*. <https://doi.org/10.15392/bjrs.v7i2A.565>

**Publisher's Note** Springer Nature remains neutral with regard to jurisdictional claims in published maps and institutional affiliations.